Report
P-16-06
February 2016

Investigation of parameters influencing bentonite block quality

Laboratory investigation

Torbjörn Sandén
Ulf Nilsson
Linus Andersson

SVENSK KÄRNBRÄNSLEHANTERING AB

SWEDISH NUCLEAR FUEL
AND WASTE MANAGEMENT CO

Box 250, SE-101 24 Stockholm
Phone +46 8 459 84 00
skb.se

SVENSK KÄRNBRÄNSLEHANTERING

ISSN 1651-4416
SKB P-16-06
ID 1466596

February 2016

Investigation of parameters influencing bentonite block quality

Laboratory investigation

Torbjörn Sandén, Ulf Nilsson, Linus Andersson
Clay Technology AB

Keywords: Granule size distribution, Grain density, Block tensile strength, Relative humidity, KBP1009.

Abstract

This report describes laboratory investigations made in order to study how different material parameters influence the achieved backfill block quality. In addition an investigation aiming to study the influence of different relative humidity in the surrounding air on the backfill blocks has been performed. The following have been investigated and/or determined:

- Granule size distribution of the raw material used for block compaction.
- Determination of the grain density.
- Determination of the dry density of individual granules.
- Determination of the tensile strength of backfill blocks and how the strength is influenced of granule size distribution, water content and density (void ratio).
- Relative humidity induced cracking on backfill blocks for different block surface properties.

In the performed tests, the following bentonite materials have been used:

- MX-80 from Wyoming USA, batches from 2002 and 2012.
- SPV200 from Wyoming USA, old batch from storage (Clay Technology AB).
- Ibeco RWC-BF, batch from 2011.
- Asha NW BFL-L, batches from 2010 and 2012.

The Asha bentonites have a grain density significant higher than the other materials. The high grain density of these materials is attributed to the high iron content. The average grain density for Asha 2010 was determined to 2888 kg/m^3 and for Asha 2012 to 2912 kg/m^3. This should be compared to 2806 kg/m^3 for Ibeco 2011 and 2802–2809 kg/m^3 for the two MX-80 batches. The average grain density for SPV200 was lower, 2658 kg/m^3, which indicates that this bentonite has another origin than the MX-80 bentonite or that there are processes separating material with different properties.

The highest granule dry density was found on the crushed MX-80 pellets, 1820 kg/m^3. Granules from the two Asha batches had a granule dry density between 1764 to 1786 kg/m^3 in average. The Ibeco 2011 bentonite had the lowest granule dry density, 1618 kg/m^3.

From the performed beam tests it was concluded that the three parameters investigated, granule size distribution, dry density (void ratio) and water content all are strongly influencing the achieved block strength.

The tested materials have large differences in density of the solids. This means that if one wants to study the influence of the void volume relative the volume of the solids on the achieved tensile strength, the tensile strength should be plotted versus the void ratio. E.g. when comparing MX-80 and Asha (density of solids of 2800 and 2910 kg/m^3 respectively) for a block dry density of 1700 kg/m^3 the difference in void ratio is approximately 10 %.

The tests show that it is favourable to crush the materials in order to increase the block strength at least at higher void ratios. The achieved strength of the blocks made from crushed material seems to be less dependent of the water content than the uncrushed materials. However, in order to facilitate the handling of the bulk material e.g. regarding dust, it is probably favourable to increase the water content somewhat.

When the compacted specimens were exposed to different relative humidity there was no evident influence of previous treatment of the exposed surfaces (standard, machined or greased) regarding the water uptake detected during the test time. The initial water content of the specimens is, however, an important factor for the behavior when exposed to different relative humidity regarding cracking and stability.

Sammanfattning

Denna rapport beskriver de laboratorieundersökningar som genomförts för att studera hur olika materialparameterar påverkar den erhållna kvaliteten på återfyllningsblock. Det har även gjorts en undersökning med syftet att studera hur olika relativ fuktighet i den omgivande luften påverkar återfyllningsblocken. Följande undersökningar och bestämningar har gjorts:

- Bestämning av granulstorleksfördelningen hos olika återfyllningsmaterial som är planerat att användas för blocktillverkning.
- Bestämning av korndensitet.
- Bestämning av granuldensitet.
- Bestämning av böjhållfastheten hos återfyllningsblock och hur denna påverkas av granulstorleksfördelning, vatteninnehåll och densitet (portal).
- Inverkan på blockens kvalitet av olika relativ fuktighet i den omgivande luften samt av blockytans egenskaper.

I testerna har följande bentoniter använts:

- MX-80 från Wyoming i USA, leverans 2002 and 2012.
- SPV200 från Wyoming USA, gammal leverans från lager (Clay Technology AB).
- Ibeco RWC-BF, leverans från 2011.
- Asha NW BFL-L, leverans från 2010 and 2012.

Korndensiteten hos bentoniten från Asha var som väntat märkbart högre än hos de andra materialen. Detta beror främst på det höga järninnehållet i denna bentonit. Medelkorndensiteten hos Asha 2010 bestämdes till 2888 kg/m^3 och för Asha 2012 till 2912 kg/m^3. Motsvarande korndesnitet för Ibeco 2011 bestämdes till 2806 kg/m^3 och för de två leveranserna av MX-80 till ca 2802–2809 kg/m^3. Medelkorndensiteten hos SPV200 bentoniten var betydligt lägre, 2658 kg/m^3. Detta indikerar att denna bentonit inte har samma ursprung som MX-80 eller att processen hos leverantören separerar material med olika egenskaper.

Den högsta granuldensiteten fanns hos det krossade pelletsmaterialet från MX-80, 1820 kg/m^3. Bentoniterna från Asha hade en medelgranuldensitet på mellan Asha 1764 och 1786 kg/m^3. Lägst granuldensitet fanns hos Ibeco 2011 med i medeltal 1618 kg/m^3.

Från blockhållfasthetstesterna kunde man dra slutsatsen att de tre parametrar som undersökts, granulstorleksfördelning, torrdensitet (portal) och vatteninnehåll, alla hade stor inverkan på vilken blockhållfasthet som erhölls.

Det är stor skillnad mellan de testade materialen när det gäller korndensiteten. Detta betyder att om man vill studera hur porvolymen relativt volymen av den fasta massan påverkar hållfastheten hos blocken måste den erhållna hållfastheten plottas mot portalet. T.ex. när man jämför MX-80 och Asha där korndensiteten är 2800 respektive 2910 kg/m^3., för en blockdensitet på 1700 kg/m^3 kommer skillnaden i portal att vara ca 10 %.

Testerna visar också att det är fördelaktigt att krossa materialet för att öka hållfastheten, särskilt vid höga portal. Den erhållna hållfastheten hos blocken tillverkade av krossad bentonit verkar också vara mindre beroende av vatteninnehållet jämfört med den okrossade bentoniten. För att underlätta hanteringen av bulkmaterialet när det gäller t.ex. dammbildning är det dock fördelaktigt att öka vatteninnehållet något.

Resultaten från testerna där de kompakterade proven exponerades för olika relativ fuktighet visar att det inte finns någon tydlig inverkan av hur den exponerade blockytan har förbehandlats (standard, maskinbearbetad eller smörjts) när det gäller det vattenupptag som har uppmätts under testtiden. Det initiala vatteninnehållet hos provkropparna är emellertid en viktig faktor när det gäller hur blocken påverkas av den omgivande relativa fuktigheten när det gäller sprickbildning och stabilitet.

Contents

1 Introduction

Compaction of bentonite powder (granules) to blocks of different sizes and shapes is an important part in the development work of different concepts for a final repository for spent nuclear fuel. The most important properties of the blocks are (except montmorillonite content and long term stability of the bentonite):

1. The desired dry density. Swelling pressure and hydraulic conductivity are functions of the dry density of the bentonite.
2. Block quality. The blocks will probably be handled with a vacuum lift tool during emplacement in a deposition hole or when it is stacked by a robot which means that there shouldn't be any cracks and the mechanical strength must be high enough. Pieces are not allowed to fall off during the installation.
3. Block storage. It must be possible to store the blocks for a certain time or expose them for different climates e.g. during the installation work without falling apart due to cracking.

Block manufacturing tests have been performed a number of times in different scales and it is known that there are a lot of parameters that are influencing the achieved block quality and the block properties (Sandén et al. 2015). The aim with this work was to investigate and determine some of the most important parameters identified:

- Influence of granule size distribution on achieved block quality (granules are conglomerates built up by finer grains).
- Determine the density of the granules for three different materials.
- Determine the grain density of three different materials (when granules are dispersed in water all grains building up a granule will be dissolved).
- Investigate the achieved block strength.
- Investigate the block behavior when exposed for different relative humidity.

2 Materials

2.1 General

The bentonite materials described and tested in this report have all been used in different tests financed by SKB. MX-80 from Wyoming, USA, has for long time been considered as a suitable bentonite for the buffer i.e. it has fulfilled the requirements for the buffer material. Asha from India and Ibeco from Greece have both been candidate materials for the backfilling of deposition tunnels. A comprehensive material investigation has been made with material from the batches delivered from Asha and Ibeco (Sandén et al. 2014).

For both MX-80 and Asha materials, two different batches have been tested.

2.2 Bentonite materials tested

The following materials have been included in the test matrix:

1. **Ibeco RWC-BF 2011** (in the report abbreviated to Ibeco) is a material that origin from Milos in Greece. Ibeco is the name of the company delivering the material, RWC stands for Radioactive Waste Clay and BF stands for BackFill. It is a natural calcium bentonite with medium montmorillonite content.
2. **Asha NW BFL-L 2010** (in the report abbreviated to Asha 2010) is produced by ASHApura Minechem Co. The material is quarried in the Kutch area on the northwest coast of India. The material is sodium dominated with a montmorillonite content of about 70 %.
3. **Asha NW BFL-L 2012** (in the report abbreviated to Asha 2012). Same material as described above, but a different batch where the granules had been crushed in order to achieve a more suitable granule size distribution.
4. **MX-80 2002**. This is a bentonite from Wyoming, USA. The material is produced by American Colloid Co. It is a natural sodium bentonite with a high content of montmorillonite. The material tested was taken from the storage at Clay Technology AB.
5. **MX-80 2012**. Same material as described above but from a batch delivered in 2012.
6. **SPV 200**. Bentonite produced by American Colloid Co and originating from the same source as MX-80 but milled to fine powder. The material tested was taken from the storage at Clay Technology AB.

2.3 Material processing

2.3.1 General

In order to achieve materials with the same origin but with different granule size distribution the as-delivered materials have been both sieved and/or milled.

2.3.2 Ibeco RWC-BF 2011

In order to achieve materials for the planned tests, samples were picked out from the as-delivered raw material, and was then either milled or sieved. The tests performed have included the following variants (Figure 2-1):

- **As-delivered**.
- **Milled**. The material was milled to fine powder. Equipment: Retsch PM 100 Ball mill. (250 rpm, 5 minutes)
- **Sieved**. All material finer than 1 mm was removed by sieving.

Figure 2-1. *Photo showing the different Ibeco materials.*

2.3.3 Asha NW BFL-L 2010 and 2012

From the as-delivered materials, samples were picked out for tests from both batches. In order to achieve materials with other granule size distribution, samples were picked out from the batch 2010, and was then either milled or sieved. The tests performed have included the following variants (Figure 2-2):

- As-delivered. Batch 2010 and 2012.
- Milled. Batch 2010. The material was milled to fine powder. Equipment: Retsch PM 100 Ball mill. (250 rpm, 5 minutes)
- Sieving. Batch 2010. All material finer than 1 mm was removed by sieving.

Figure 2-2. *Photo showing the different Asha materials.*

2.3.4 MX-80 2002 and 2012

From the as-delivered materials samples were picked out for tests from both batches. In order to achieve materials with other granule size distribution an older batch of SPV 200 (bentonite from the same source but milled) was included in the test series. The coarser material was achieved by crushing MX-80 pellet (roller compacted to pillow shape) and then removes the fines. The tests performed have included the following variants (Figure 2-3):

- As-delivered I. MX-80: Batch 2002 and 2012.
- As-delivered II. SPV 200.
- Crushing. Compacted pillow shaped pellet made of MX-80 were crushed mechanically. All material finer than 1 mm was removed by sieving.

Figure 2-3. *Photo showing the different MX-80 materials.*

3 Granule size distribution

3.1 General

The granule size distribution was determined for all materials included in this investigation.

3.1.1 Method

Samples were picked out from each of the selected materials. The total sample weight was approx. 200 g for the crushed materials and approx. 500 g for the coarser materials.

The sieving was made using standard sieves but instead of using the vibrator the sieving was done manually in order to avoid crushing of the granules. This is not a standard method but since the interesting part was the size of the granules and not of the individual grain, this was assessed to be the most suitable method.

3.1.2 Results

The results from the determination of the granule size distribution are presented in Figure 3-1 to 3-3. The two batches from Asha have a very similar granule size distribution although the batch from 2012 was ordered as a crushed material with a maximum granule size of 3 mm. A visual inspection indicated that the material had been crushed between two rollers with a gap spacing of ~3 mm. This procedure had disintegrated, or reshaped, the large granules but at the same time new granules had been formed with a thickness of 3 mm and of various lengths and widths. This is the explanation for the similar granule size distribution determined for the two batches. The newly formed granules seemed however, due to the fact that they were softer, to affect the compaction properties and it was observed that the achieved block quality was improved.

The milled Asha and Ibeco had a similar granule size distribution. All granules had after milling a size smaller than 1 mm. The SPV 200 was the finest material with approx. 80 % finer than 0.1 mm.

The two batches of MX-80 from 2002 and 2012 had a very similar granule size distribution.

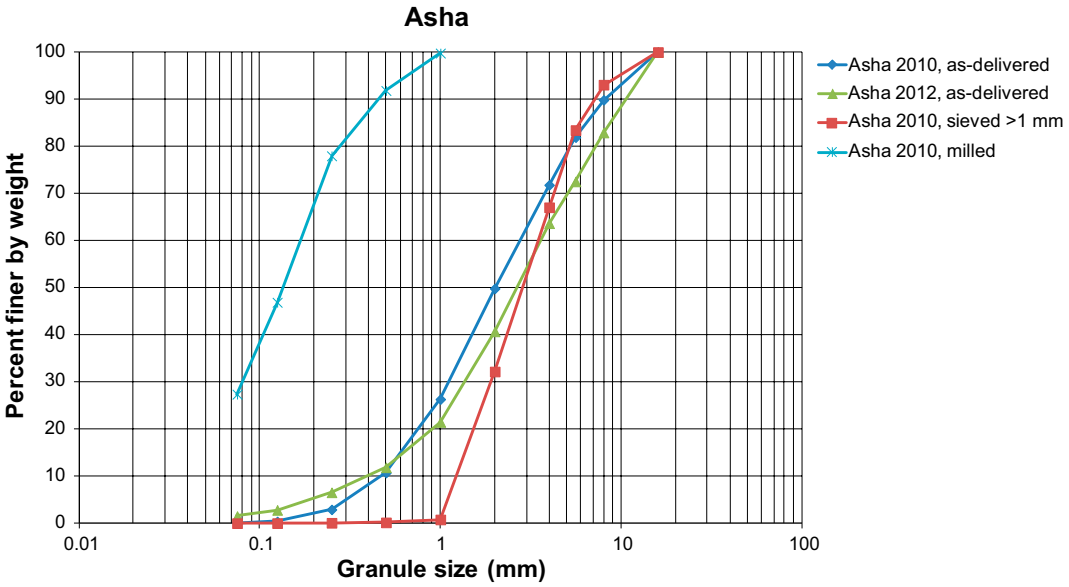

Figure 3-1. *Granule size distribution for the Asha materials.*

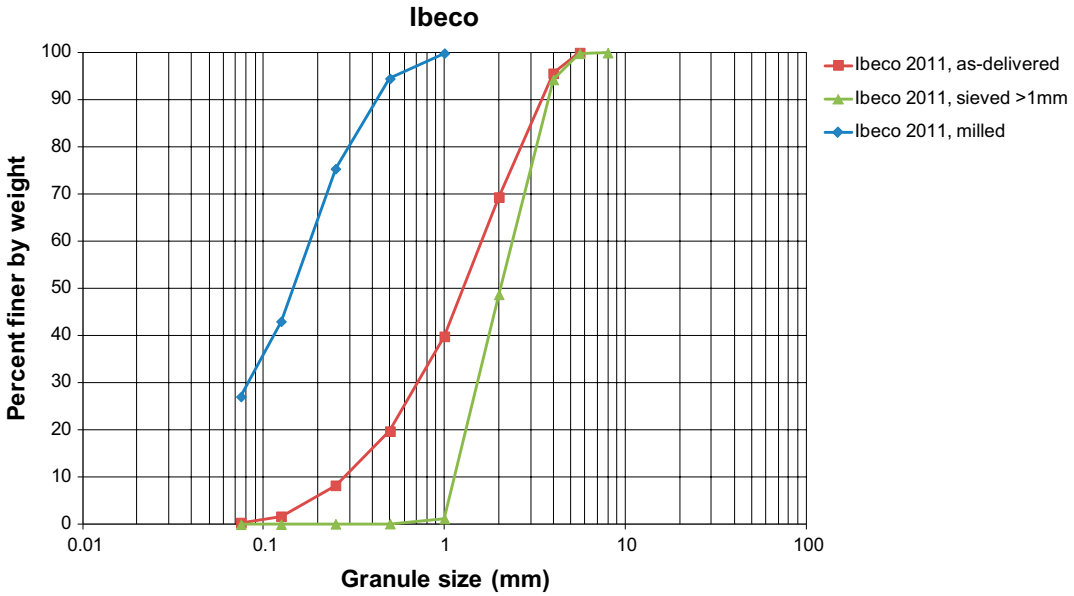

Figure 3-2. *Granule size distribution for the Ibeco materials.*

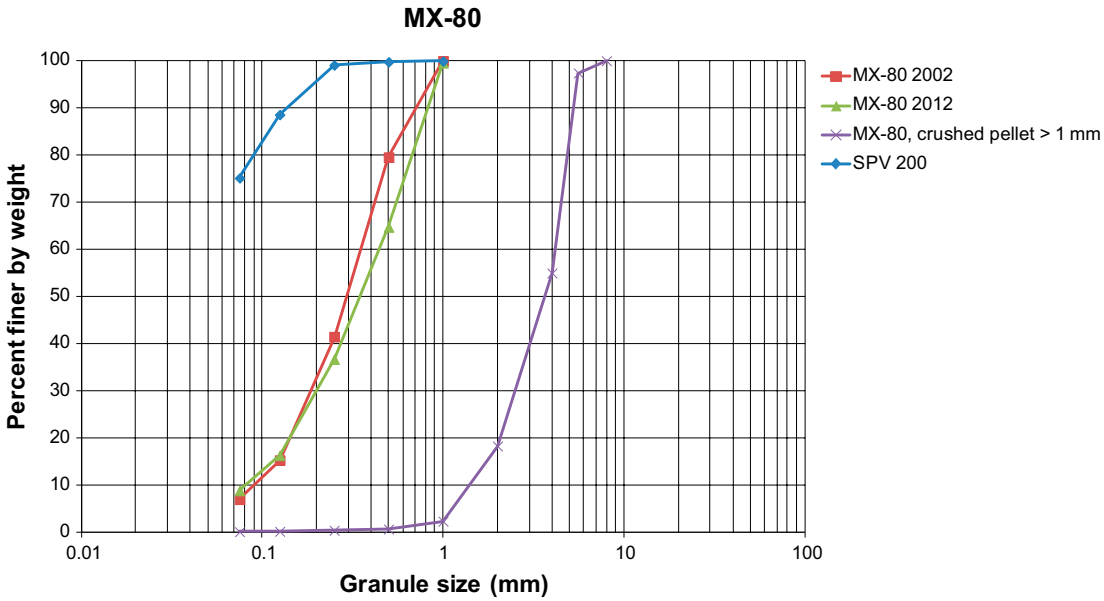

Figure 3-3. *Granule size distribution for the MX-80 materials.*

4 Grain density

4.1 General

The grain density of a material is needed to calculate e.g. the degree of saturation and the void ratio.

4.2 Method

The grain density of the bentonite materials was determined by use of volumetric flasks. After determining the volume of the flasks very carefully, dried material was mixed with 1 M NaCl solution in order to prevent swelling of the bentonite. When the mass of the solids, the total volume, the total mass (solids and flask) and the density of the liquid are known, it is possible to calculate the grain density of the material. The method is described in detail in Karnland et al. (2006).

The materials were before measurements milled according to description in Section 2.3.

4.3 Test matrix

The grain density was determined on five different samples for each of the following materials/batches:

1. MX-80 2002
2. MX-80 2012
3. SPV200 (Old batch from Clay Technology's store)
4. Ibeco 2011
5. Asha 2010.
6. Asha 2012.

4.4 Results

The results of the measurements are provided in Table 4-1. The grain density of the Asha materials is as expected significant higher than the other materials. The high grain density of these materials is attributed to the high iron content (Sandén et al. 2014). The average grain density for Ibeco 2011 was 2806 kg/m^3 which is higher than in earlier investigations with this material e.g. in Sandén et al. (2014) where it was determined to 2723 kg/m^3. A difference can be that in this investigation all materials tested were milled before the measurements. The determined average grain density of material from the two MX-80 batches was almost the same, between 2802–2809 kg/m^3. This is very close to the grain density often used for this material (2780–2790 kg/m^3). The grain density of the SPV200 material was considerably lower with an average of 2658 kg/m^3. This indicates that the origin of this material is not the same as the MX-80.

Table 4-1. Compilation of data from the determinations of grain density.

Material	Sample 1 kg/m^3	Sample 2 kg/m^3	Sample 3 kg/m^3	Sample 4 kg/m^3	Sample 5 kg/m^3	Average kg/m^3	Standard dev. kg/m^3
MX-80 2002	2769	2814	2831	2804	2791	2802	23.7
MX-80 2012	2830	2782	2825	2827	2779	2809	25.9
SPV200	2610	2695	2649	2674	2664	2658	31.6
Ibeco RWC BF 2011	2794	2824	2813	2804	2796	2806	12.6
Asha 2010	2872	2864	2898	2934	2870	2888	29.1
Asha 2012	2883	2943	2883	2923	2927	2912	27.1

5 Density of granules

5.1 General

The density and strength of the individual granules is believed to influence the final block quality regarding evenness of surfaces and the stability of edges. It is also possible that the strength of the manufactured block is influenced.

5.2 Method

The density of individual granules was determined for the as-delivered Asha, the as-delivered Ibeco and for MX-80. For the Asha and Ibeco materials it was possible to pick out individual granules from the as-delivered material while for the MX-80 material the samples were picked out from the crushed pellets. The granule size of the picked out samples varied between 2 and 5 mm.

A number of granules were places in a small basket, see photo provided in Figure 5-1. The weight of the basket was less than 0.1 g and the weight of the granules was between 1 and 3 g.

The bulk density was determined by hanging the basket containing a number of granules in a thin thread under a balance. The sample was then weighed, first in air (m_b) and then submerged into paraffin oil (m_{bp}) with known density (ρ_p). In all calculations, it was compensated for the weight of the basket and the thread. The volume of the sample was calculated according to the following:

$$V = \frac{(m_b - m_{bp})}{\rho_p} \qquad \text{(Equation 5-1)}$$

where ρ_p is the paraffin oil density. The bulk density of the sample was then calculated:

$$\rho_b = \frac{m_b}{V} \qquad \text{(Equation 5-2)}$$

After determining the water content and the bulk density of each sample it was possible to calculate the dry density (ρ_d):

$$\rho_d = \frac{\rho_b}{1 + w} \qquad \text{(Equation 5-3)}$$

The void ratio e may be calculated from the density of the clay solids δ_s and the dry density δ_d according to:

$$e = \frac{\delta_s}{\delta_d} - 1 \qquad \text{(Equation 5-4)}$$

Figure 5-1. *Photo showing the basket containing a number of granules.*

5.3 Results

The granules from the different materials tested have rather different shapes; see photos provided in Figure 5-2 to 5-5.

- Asha 2010 batch. The granules are angular and seem to be very hard.
- Asha 2012. The granules are flat (see description in Section 3.1.2) and seems to be softer than the ones from 2010.
- Ibeco 2011. The granules are smaller and rather soft.
- MX-80. The granules are angular and seem to be rather stiff.

A compilation of the results from the density determinations are provided in Figure 5-6 and in Table 5-1.

Figure 5-2. *Close up of the granules in the as-delivered material from the Asha 2010 batch.*

Figure 5-3. *Photos showing the difference in granule shape between Asha 2010 and Asha 2012.*
Left: *Close up of the Asha 2010 material* ***Right:*** *Close up of the Asha 2012 material.*

Figure 5-4. *Close up of the granules in the as-delivered material from the Ibeco 2011 batch.*

Figure 5-5. Close up of the granules of crushed MX-80 pellets.

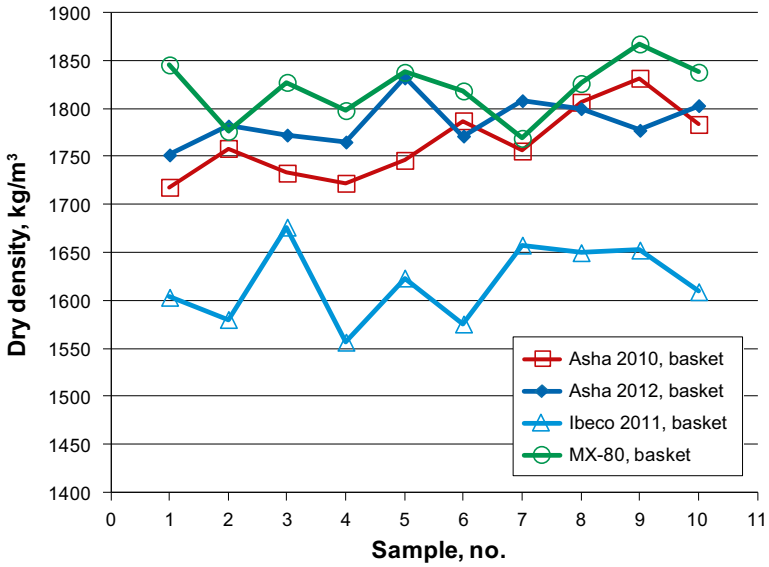

Figure 5-6. The determined dry density plotted versus sample number for the three materials.

Table 5-1. Compilation of data from the determinations of the dry density of the different granule types.

Sample no.	Asha 2010 kg/m³	Asha 2012 kg/m³	Ibeco 2011 kg/m³	MX-80 kg/m³
1	1718	1752	1603	1845
2	1758	1782	1580	1776
3	1733	1772	1676	1827
4	1722	1765	1557	1798
5	1746	1832	1623	1838
6	1787	1771	1576	1818
7	1756	1808	1658	1769
8	1806	1800	1650	1826
9	1831	1777	1653	1867
10	1783	1803	1609	1838
Min. granule density, kg/m³	**1718**	**1752**	**1557**	**1769**
Max. granule density, kg/m³	**1831**	**1808**	**1676**	**1867**
Average density, kg/m³	**1764**	**1786**	**1618**	**1820**
Standard dev., kg/m³	**37.3**	**24.0**	**40.1**	**30.9**

6 Block quality and strength

6.1 General

In order to check if a certain material is suitable for block manufacturing and how different material parameters such as granule size distribution, water content and density affects the strength of the blocks, so-called beam tests have been performed.

The compaction of specimens and the following sawing will also give information regarding e.g. the brittleness of the edges.

6.2 Method

The specimen preparation was made according to the following:

- Small specimens were compacted in laboratory (approx. Ø 50 mm, h 20 mm). From each of these specimens beams were sawn out (axbxc ~10×20×35 mm^3).
- The beams were forced to failure by applying a constant deformation rate of 0.10 mm/min at the middle of the beam. The load and the displacement were measured continuously; see drawing and photo provided in Figure 6-1.

The tensile stress (σ_t) and the tensile strain (ε_t) were evaluated with the following equations (see Figure 5-11).

$$\sigma_t = \frac{6Qc}{4ba^2} \qquad \text{(Equation 6-1)}$$

$$\varepsilon_t = \frac{a\omega 6}{c^2} \qquad \text{(Equation 6-2)}$$

where

Q = vertical force

a = specimen height

b = specimen width

c = the length between the support points

ω = the vertical displacement at the middle of the beam

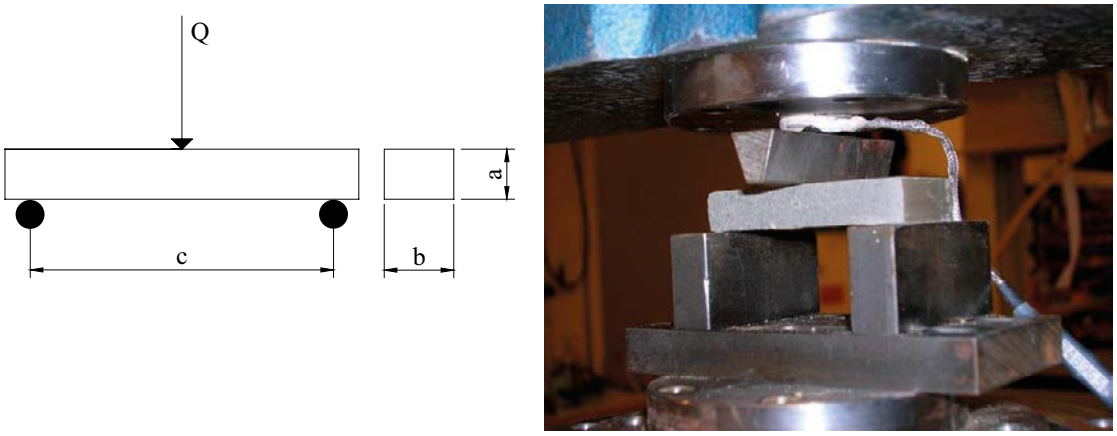

Figure 6-1. *Test arrangement for determination of the tensile strength.*

6.3 Test matrix

The performed tests were divided in two phases:

1. A large test matrix including three materials, different granule sizes, different batches, different water contents and two different compaction pressures is shown in Table 6-1. This test series included 66 different specimens and from each of these, two beams were sawed out i.e. in total 132 beam tests were made.
2. A smaller test matrix including two materials, two granule sizes, one water content and six different compaction pressures is shown in Table 6-2. This test series included 24 different specimens and from each of these, two beams were sawed out i.e. in total 48 beam tests were made.

Table 6-1. The complete test matrix for test series 1.

Asha , 25 MPa				
Water content	**Crushed**	**Batch 2010**	**Batch 2012**	**Granules (>1 mm)**
17 %	Asha_25_17_1	Asha_25_17_2	Asha_25_17_3	Asha_25_17_4
20 %	Asha_25_20_1	Asha_25_20_2	Asha_25_20_3	Asha_25_20_4
22 %	Asha_25_22_1	Asha_25_22_2	Asha_25_22_3	Asha_25_22_4

Asha , 50 MPa				
Water content	**Crushed**	**Batch 2010**	**Batch 2012**	**Granules (>1 mm)**
17 %	Asha_50_17_1	Asha_50_17_2	Asha_50_17_3	Asha_50_17_4
20 %	Asha_50_20_1	Asha_50_20_2	Asha_50_20_3	Asha_50_20_4
22 %	Asha_50_22_1	Asha_50_22_2	Asha_50_22_3	Asha_50_22_4

IBECO 2011, 25 MPa			
Water content	**Crushed**	**As-delivered**	**Granules (>1 mm)**
17 %	Ibeco_25_17_1	Ibeco_25_17_2	Ibeco_25_17_3
20 %	Ibeco_25_20_1	Ibeco_25_20_2	Ibeco_25_20_3
22 %	Ibeco_25_22_1	Ibeco_25_22_2	Ibeco_25_22_3

IBECO 2011, 50 MPa			
Water content	**Crushed**	**As-delivered**	**Granules (>1 mm)**
17 %	Ibeco_50_17_1	Ibeco_50_17_2	Ibeco_50_17_3
20 %	Ibeco_50_20_1	Ibeco_50_20_2	Ibeco_50_20_3
22 %	Ibeco_50_22_1	Ibeco_50_22_2	Ibeco_50_22_3

MX-80, 25 MPa				
Water content	**SPV200 (old batch)**	**Batch 2002**	**Batch 2012**	**Granules (>1 mm)**
12 %	MX-80_25_12_1	MX-80_25_12_2	MX-80_25_12_3	MX-80_25_12_4
17 %	MX-80_25_17_1	MX-80_25_17_2	MX-80_25_17_3	MX-80_25_17_4
21 %	MX-80__25_21_1	MX-80__25_21_2	MX-80__25_21_3	MX-80__25_21_4

MX-80, 50 MPa				
Water content	**SPV200 (old batch)**	**Batch 2002**	**Batch 2012**	**Granules (>1 mm)**
12 %	MX-80_50_12_1	MX-80_50_12_2	MX-80_50_12_3	MX-80_50_12_4
17 %	MX-80_50_17_1	MX-80_50_17_2	MX-80_50_17_3	MX-80_50_17_4
21 %	MX-80_50_21_1	MX-80_50_21_2	MX-80_50_21_3	MX-80_50_21_4

Table 6-2. The complete test matrix for test series 2.

	Asha		MX-80	
Compaction pressure	**Crushed**	**Granules (>1 mm)**	**SPV 200**	**Granules (>1 mm)**
20 MPa	Asha_20_17_1	Asha_20_17_4	MX-80_20_17_1	MX-80_20_17_4
25 MPa	Asha_25_17_1	Asha_25_17_4	MX-80_25_17_1	MX-80_25_17_4
30 MPa	Asha_30_17_1	Asha_30_17_4	MX-80_30_17_1	MX-80_30_17_4
35 MPa	Asha_35_17_1	Asha_35_17_4	MX-80_35_17_1	MX-80_35_17_4
40 MPa	Asha_40_17_1	Asha_40_17_4	MX-80_40_17_1	MX-80_40_17_4
50 MPa	Asha_50_17_1	Asha_50_17_4	MX-80_50_17_1	MX-80_50_17_4

6.4 Results

6.4.1 Compaction of specimens

The specimens were compacted in laboratory according to the test matrix provided in Section 6-3. After compaction, photos were taken of all specimens; see Figure 6-2, 6-3 and Appendix 1 to 5.

The photos show the big differences in the specimen texture depending on the granule size and on the water content.

6.4.2 Sawing out beams

Two beams were sawed out from each of the compacted specimens. Photos of the beams are provided in Figure 6-4, 6-5 and in Appendix 6 to 10. As shown in the photos, most of the beams were sawed out without any problems. However, a few specimens were rather brittle and it was not possible to achieve beams of good quality. This problem occurred for Asha and Ibeco specimens with the lowest water content and with large granules.

After having performed the strength tests the pieces of the beam were used to determine the density and water content.

Figure 6-2. *Photo showing Asha specimens compacted with 25 MPa.*

Figure 6-3. *Photo showing Asha specimens compacted with 50 MPa.*

Figure 6-4. *Photo showing beams of Asha specimens compacted with 25 MPa.*

Figure 6-5. *Photo showing beams of Asha specimens compacted with 50 MPa.*

6.4.3 Determined block strength

The results from the tests performed with Asha material in test series 1 are presented in Table 6-3. The results from the other materials are provided in Appendix 10 to 12.

The investigation have shown that for a certain material it is possible to achieve information regarding the block strength and how it is influenced by the dry density and the water content by performing so called beam tests. However, when the results should be compared with those from tests with other materials it is necessary to compare the strength plotted versus the void ratio. The void ratio is defined as the ratio between the volume of void-space and the volume of solids. For a certain dry density, the void ratio may be quite different for different materials depending on differences in the density of the clay solids, see Section 5.

The void ratio e may be calculated from the density of the clay solids δ_s and the dry density δ_d according to:

$$e = \frac{\delta_s}{\delta_d} - 1 \qquad \text{(Equation 6-3)}$$

Figure 6-6 shows the results from tests performed with ASHA granules and MX-80 granules (part of tests series 2) plotted versus the dry density. In Figure 6-7, the same data is instead plotted versus the void ratio. Figure 6-8 shows that there is an almost linear relation between tensile strength and void ratio.

It is obvious that the void ratio influences the strength of the blocks very strongly. Another parameter that also affects the tensile strength is the water content.

Table 6-3. Compilation of results from the tests performed with ASHA material in test series 1.

Test ID	Comp. Pressure MPa	Water content %	Dry density kg/m³	Void ratio	Strain at failure %	Max. tensile stress kPa
ASHA_25_17_1A	25	16.0	1719	0.687	0.698	844.6
ASHA_25_17_1B	25	16.0	1719	0.687	0.617	491.1
ASHA_25_20_1A	25	18.7	1728	0.678	0.642	1287.6
ASHA_25_20_1B	25	18.7	1728	0.678	0.724	735.9
ASHA_25_22_1A	25	20.2	1740	0.667	0.714	933.1
ASHA_25_22_1B	25	20.2	1740	0.667	0.587	1018.4
ASHA_25_17_2A	25	17.7	1708	0.698	0.712	373.9
ASHA_25_17_2B	25	17.7	1708	0.698	0.874	303.2
ASHA_25_20_2A	25	19.5	1688	0.718	0.58	214.9
ASHA_25_20_2B	25	19.5	1688	0.718	0.864	411.6
ASHA_25_22_2A	25	20.8	1712	0.694	0.88	808.4
ASHA_25_22_2B	25	20.8	1712	0.694	1.001	666.1
ASHA_25_17_3A	25	15.4	1729	0.677	0.634	177.9
ASHA_25_17_3B	25			0.000		
ASHA_25_20_3A	25	17.9	1747	0.660	0.809	580.6
ASHA_25_20_3B	25	17.9	1747	0.660	0.626	540.2
ASHA_25_22_3A	25	20.6	1689	0.717	1.024	783.5
ASHA_25_22_3B	25	20.6	1689	0.717	0.927	723.1
ASHA_25_17_4A	25	16.9	1729	0.677	0.855	174.1
ASHA_25_17_4B	25			0.000		
ASHA_25_20_4A	25	19.0	1700	0.706	0.675	386.5
ASHA_25_20_4B	25	19.0	1700	0.706	0.945	319.1
ASHA_25_22_4A	25	21.5	1713	0.693	0.694	586.7
ASHA_25_22_4B	25	21.5	1713	0.693	0.996	555.2

Test ID	Comp. Pressure MPa	Water content %	Dry density kg/m³	Void ratio	Strain at failure %	Max. tensile stress kPa
ASHA_50_17_1A	50	16.1	1839	0.577	0.472	1006
ASHA_50_17_1B	50	16.1	1839	0.577	0.643	1264
ASHA_50_20_1A	50	18.7	1816	0.597	0.607	1527
ASHA_50_20_1B	50	18.7	1816	0.597	0.53	1200
ASHA_50_22_1A	50	20.8	1787	0.623	0.92	1635
ASHA_50_22_1B	50	20.8	1787	0.623	0.845	1176
ASHA_50_17_2A	50	17.4	1814	0.599	0.683	1181
ASHA_50_17_2B	50	17.4	1814	0.599	0.917	1235
ASHA_50_20_2A	50	19.3	1778	0.631	0.753	1224
ASHA_50_20_2B	50	19.3	1778	0.631	0.778	1332
ASHA_50_22_2A	50	20.8	1756	0.651	0.63	1074
ASHA_50_22_2B	50	20.8	1756	0.651	0.967	1248
ASHA_50_17_3A	50	16.1	1813	0.600	0.874	477
ASHA_50_17_3B	50	16.1	1813	0.600	0.791	963
ASHA_50_20_3A	50	18.2	1799	0.612	0.815	1287
ASHA_50_20_3B	50	18.2	1799	0.612	0.998	1338
ASHA_50_22_3A	50	19.7	1771	0.637	0.877	1075
ASHA_50_22_3B	50	19.7	1771	0.637	0.989	925
ASHA_50_17_4A	50	16.3	1806	0.000		0
ASHA_50_17_4B	50			0.000		
ASHA_50_20_4A	50	19.6	1766	0.642	0.925	695
ASHA_50_20_4B	50	19.6	1766	0.642	0.942	753
ASHA_50_22_4A	50	21.2	1747	0.660	0.616	1134
ASHA_50_22_4B	50	21.2	1747	0.660	1.162	1179

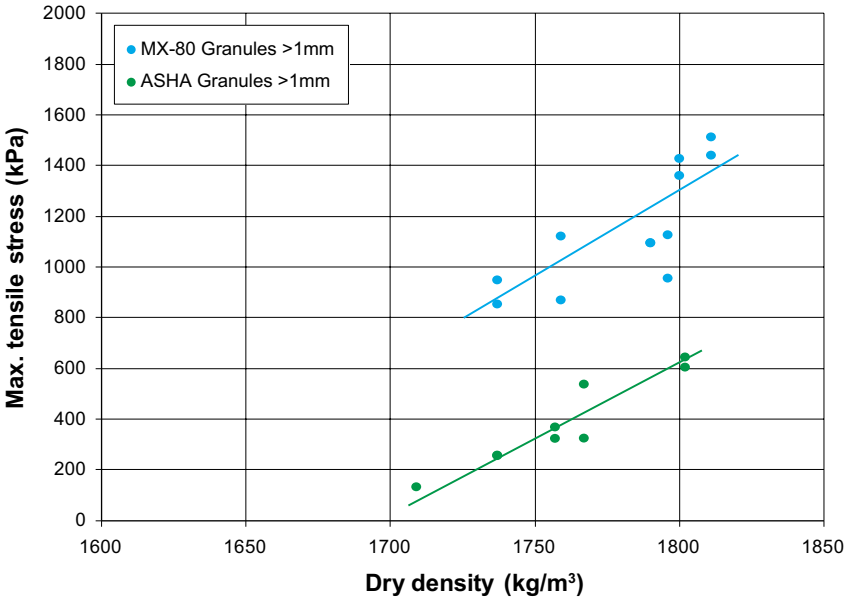

Figure 6-6. *The maximum stress plotted versus dry density for the Asha and MX-80 specimens with granules >1 mm.*

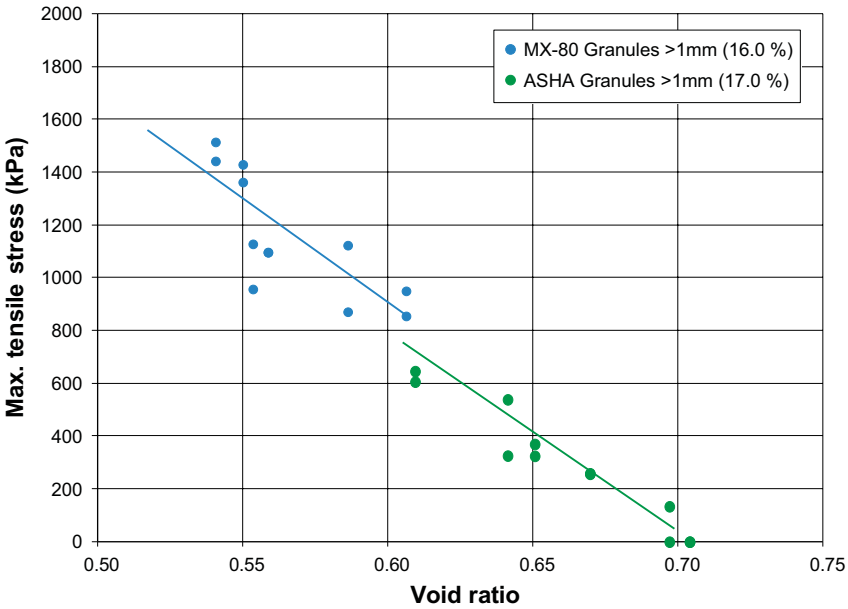

Figure 6-7. *The maximum stress plotted versus the void ratio for the Asha and MX-80 specimens with granules >1 mm.*

The results from all tests performed in test series 1 and 2 are presented in Figure 6-8 (as-delivered), 6-9 (granules) and 6-10 (crushed). The data have been plotted according to the following: Square-Ibeco, Diamond- Asha and Ball-MX-80. In addition the results have been divided into different colours depending on the water content: light blue: <14 %, blue: 14–16 %, green: 16–18 %, red: 18–20 % and dark red > 20 %.

The results from all tests performed with the as-delivered materials are presented in Figure 6-8.The data have been plotted in two graphs since the variation in granule size distribution between MX-80 and Asha /Ibeco is large, see Chapter 3, and this influences the results. The graphs show that the achieved block strength is very similar for a certain void ratio and water content for both Asha and Ibeco. The graphs also show that the influence of both void ratio and water content on the strength is very strong.

The trends from the as-delivered material are even stronger for the granules, see results provided in the Figure 6-9. The division along lines for different water contents is very clear for all three materials even if the spread in results is rather high.

The results from the tests performed with fine materials, crushed or delivered with a maximum grain size of 1 mm, are somewhat different, Figure 6-10. It seems that all results are gathered, independent of material and/or water content, along a wide band. The strength of blocks compacted with fine materials is generally higher especially for higher void ratios.

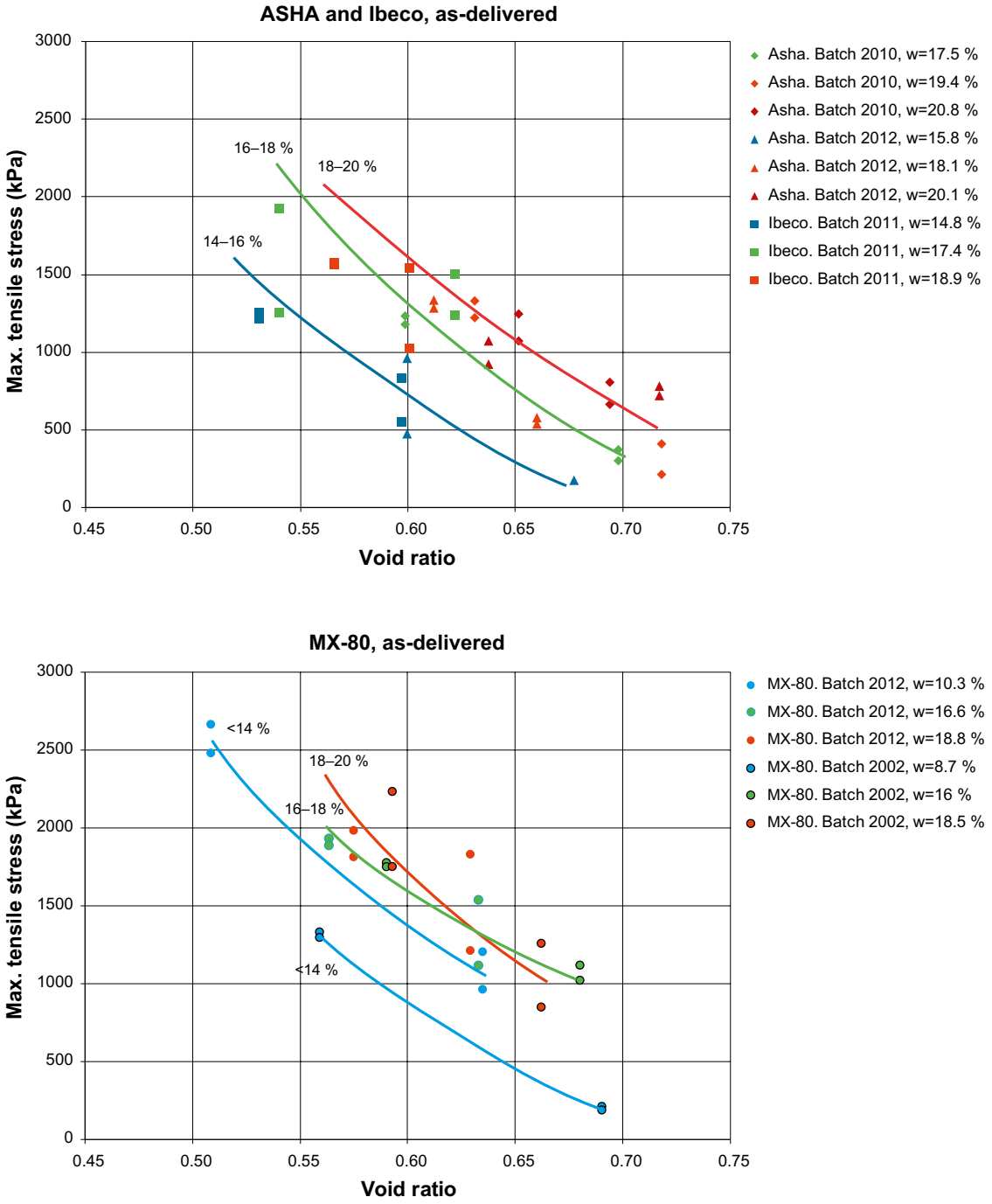

***Figure 6-8. Upper**: The determined maximum tensile strength for the as-delivered Asha and Ibeco batches plotted versus void ratio. **Lower**: The determined maximum tensile strength for the as-delivered MX-80 batches plotted versus void ratio.*

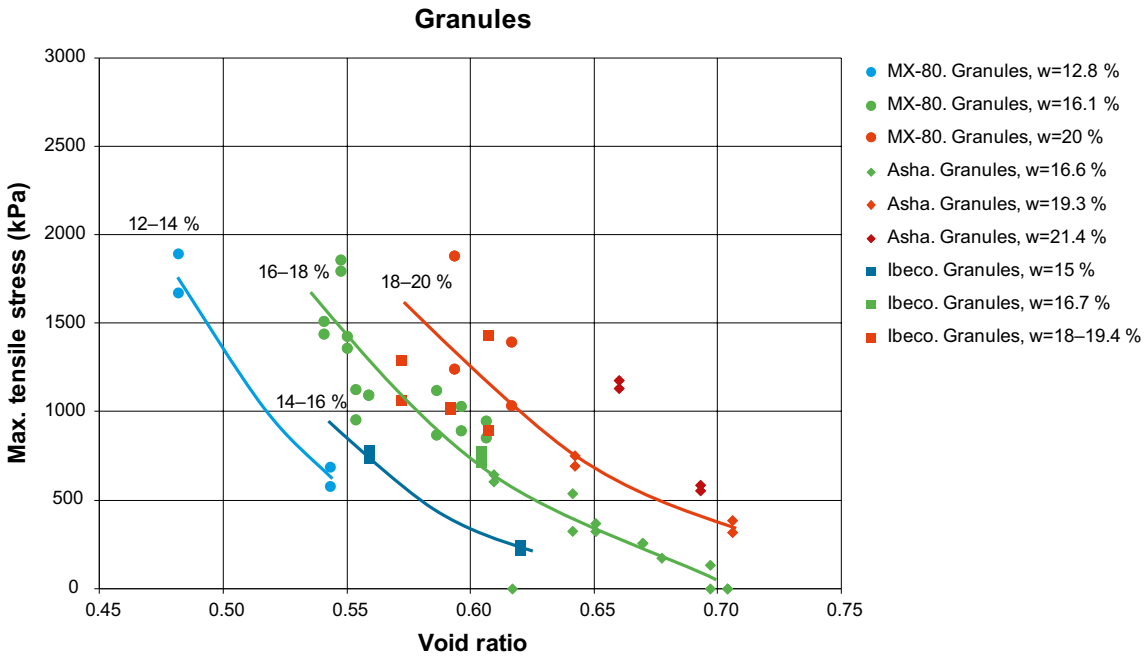

Figure 6-9. *The determined maximum tensile strength for granules larger than 1mm for all tested materials plotted versus void ratio.*

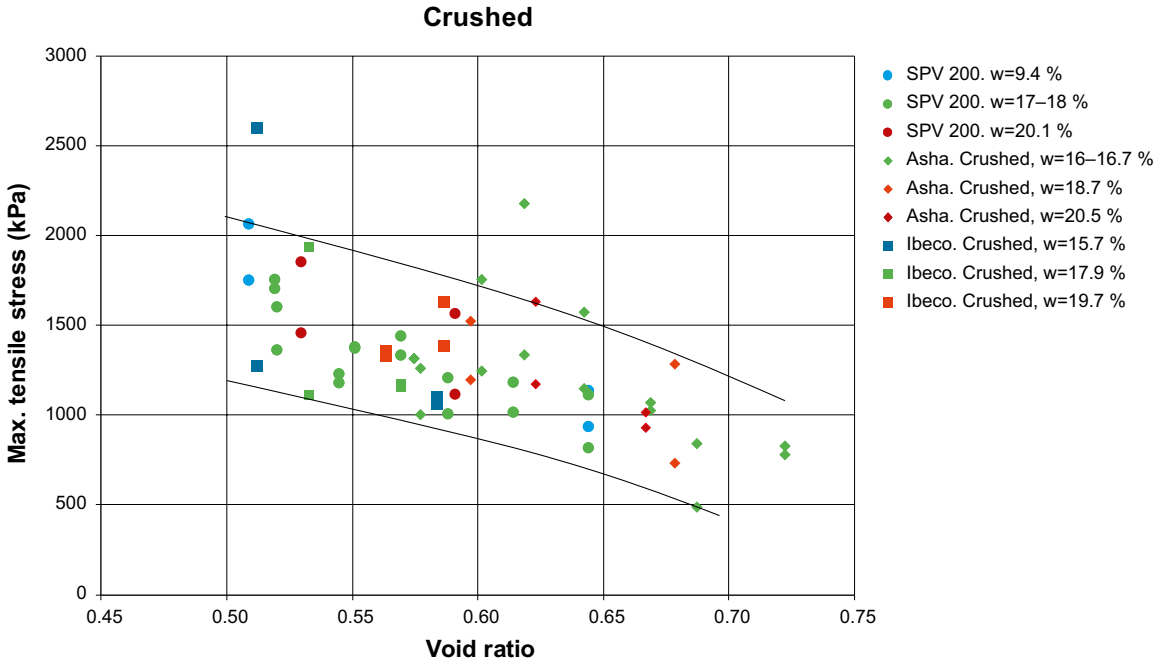

Figure 6-10. *The determined maximum tensile for the fine and crushed materials plotted versus void ratio.*

6.5 Comments and conclusions

From the performed tests the following comments and conclusions have been made:

- The three parameters investigated, granule size distribution, dry density (void ratio) and water content are all strongly influencing the achieved block strength.
- The tested materials have large differences in density of the solids. This means that if one wants to study the influence of the void volume relative the volume of the solids on the achieved tensile strength, the tensile strength should be plotted versus the void ratio. This applies especially when comparing materials with large differences regarding the density of the solids. E.g. when comparing MX-80 and Asha (density of solids of 2800 and 2910 kg/m^3 respectively) for a block dry density of 1700 kg/m^3 the difference in void ratio is approximately 10 %
- The tests show that it is favourable to crush the materials in order to increase the block strength at least at higher void ratios. The achieved strength of the crushed material seems to be less dependent of the water content than the uncrushed materials. However, in order to facilitate the handling of the bulk material e.g. regarding dust, it is probably favourable to choose a water content around 17–22 %, which is higher than the water content on the as-delivered bentonite (normally between 10–12 %).

7 Relative humidity induced cracking

7.1 General

Bentonite is a hygroscopic material i.e. it can both absorb and emit moisture from the surrounding environment. Because of the affinity for atmospheric moisture, bentonite powder or compacted blocks will require storage in sealed containers in order to not change properties.

During the installation process of bentonite blocks in a repository for radioactive waste, bentonite blocks will be exposed for atmosphere with different humidity. It is of great importance that the blocks can be lifted and handled in a safe way in order to achieve a high quality installation.

This investigation aims to increase the understanding regarding how blocks with different initial water content and density reacts when exposed to different relative humidities. The influence of machined block surfaces and the use of grease during block compaction on the ability for the blocks to take up water from the surrounding atmosphere have also been a part of the investigation.

The tests have been performed using MX-80 from the 2012 batch. Three different relative humidities were chosen for testing: 35 %, 75 % and 95 %.

7.2 Method

7.2.1 Specimen preparation

All specimens were compacted using 80.0 g material with the desired water content. A manual hydraulic press was used to compact the specimens. Figure 7-1 shows the hydraulic press, the compaction equipment and a specimen. Figure 7-2 shows all the prepared specimens. After manufacturing the specimens were packed in double layers (a tight plastic wrap and a zip-lock bag) to prevent drying. The determined dimensions and weights of all specimens after manufacturing and also after machining are found in Appendix 14.

Three types of specimens were manufactured:

- **Standard (S)**. The material was placed in the cylinder and compacted to the desired compaction pressure.
- **Machined (M)**. The compaction was performed identically to the standard procedure. After compaction the specimen was machined in a lathe on all sides. Approximately 1 mm of material was removed from each specimen.
- **Greased (G)**. A lubricant (molybdenum disulfide) is applied over all surfaces in the compaction equipment. Apart from that the compaction was performed identically to the standard procedure.

7.2.2 Test performance

A special climate chamber was used for the test. The test procedure followed an identical routine for all specimens. All 24 specimens for each of the three relative humidities were treated as one batch and placed on two trays. Results were documented through a routine with visual inspection (photos, supplemented by notes) and weighing. This was performed at specific time intervals according to the following plan:

- Test startup.
- Every two hours the first ten hours.
- Twice a day, the second and third day.
- Once every day for the remaining test time.

It is considered of great importance to have as similar time intervals as possible for documentation of the three test series. Figure 7-3 shows the arrangement with specimens on a tray.

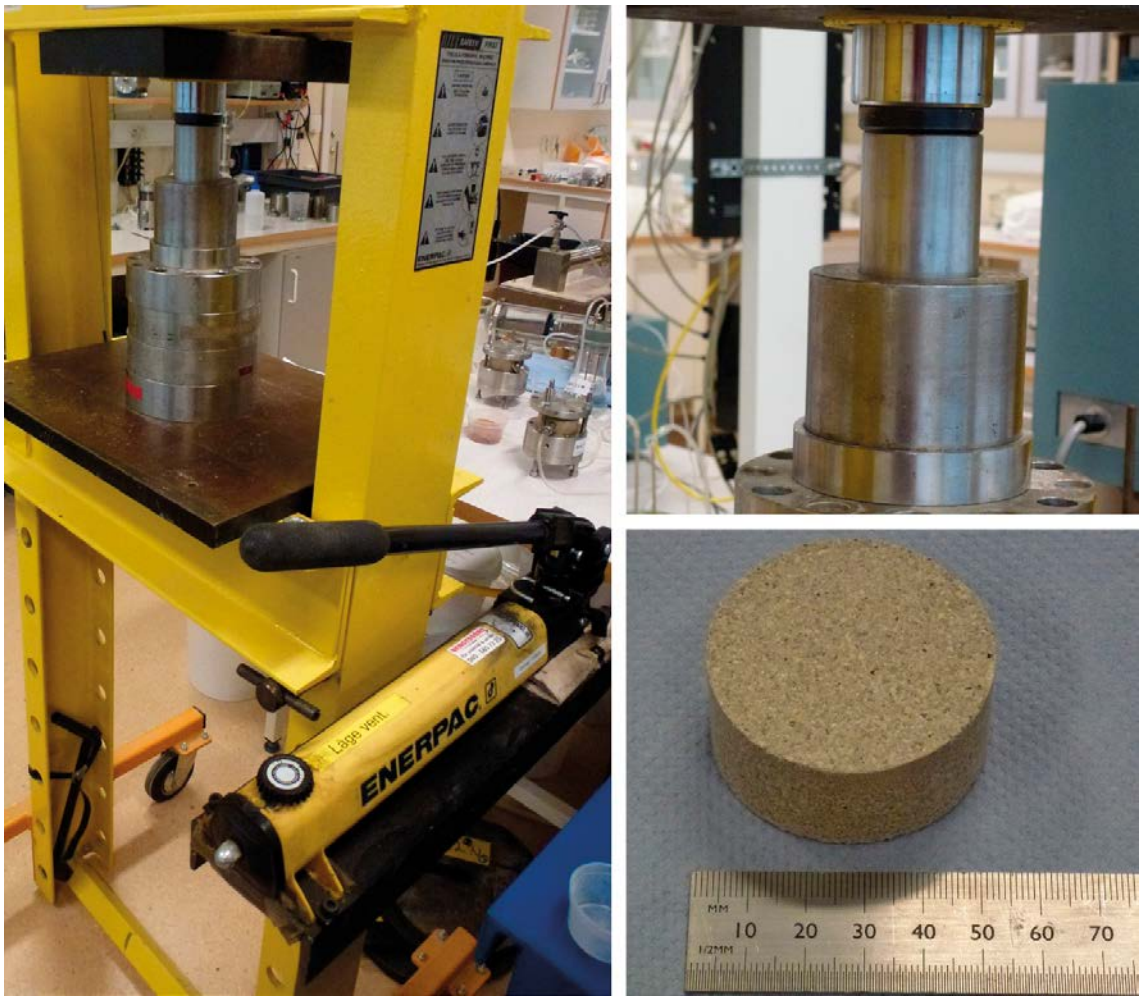

Figure 7-1. *Compaction of specimens. The hydraulic press is seen to the left. To the upper right it is seen how the piston is compressing a specimen in the compaction cylinder. A compacted specimen is seen to the lower right.*

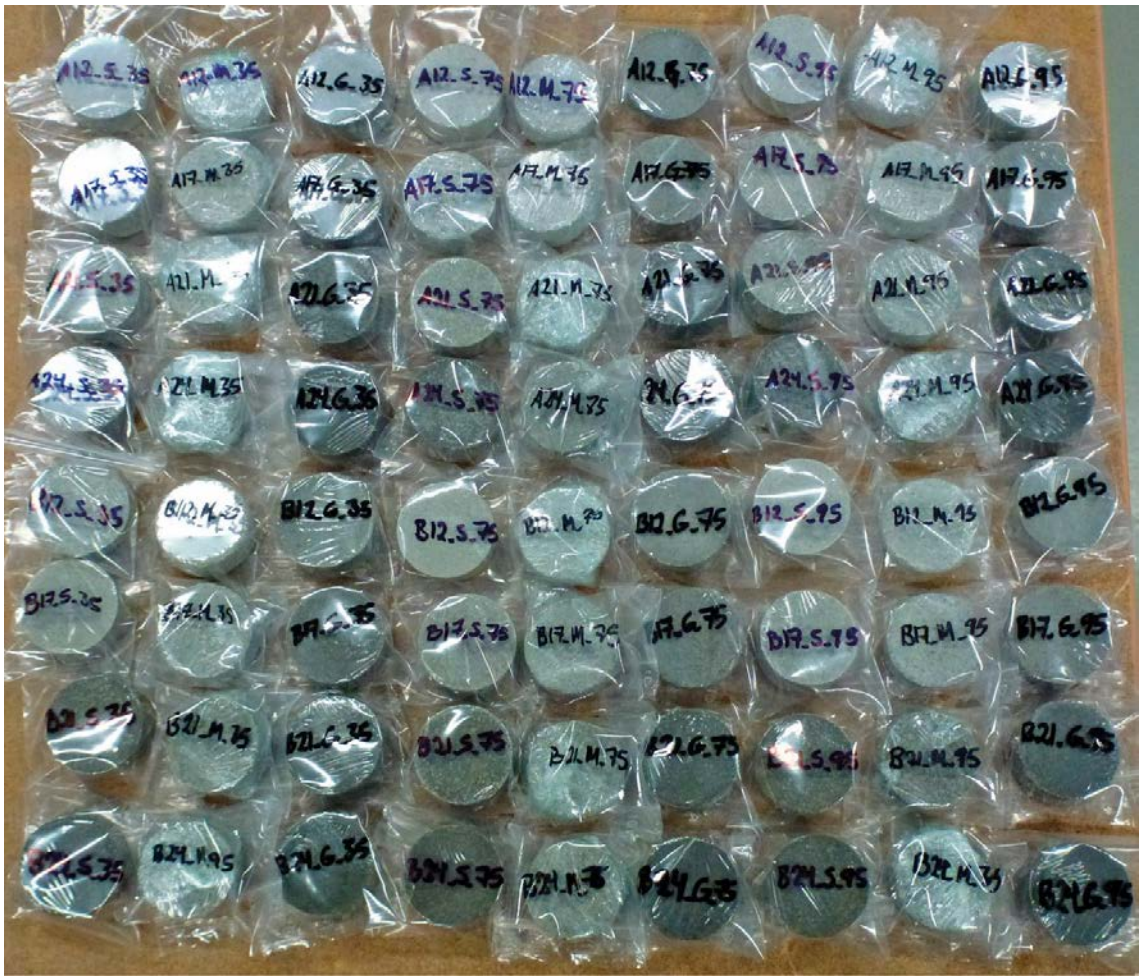

Figure 7-2. *All the prepared specimens. The specimens are packed in double plastic layers after manufacturing.*

Figure 7-3. *Photo showing specimens, each container is also marked.*

7.3 Test matrix

In order to investigate the influence of the water uptake and forming of fractures on several parameters, an extensive test matrix was established. MX-80 2012 was used in all tests. Specimens were compacted at both 25 MPa and 50 MPa compaction pressure to achieve two different densities. Four water contents were used and the specimens were prepared using three different manufacturing methods, see Section 7.2.1:

- Standard specimen
- Greased specimen
- Machined specimen

This resulted in 24 unique specimens. The specimens were to be tested at three different relative humidities. Thereby three of each specimen was prepared, resulting in a total of 72 specimens. Table 7-1 and Table 7-2 show the full test matrix.

Table 7-1. Full test matrix for the specimens prepared with 25 MPa compaction pressure.

Compaction pressure: 25 MPa					
Water content		**as-delivered**	**17 %**	**21 %**	**24 %**
RH=35 %	Standard	A12_S_35	A17_S_35	A21_S_35	A24_S_35
	Machined	A12_M_35	A17_M_35	A21_M_35	A24_M_35
	Greased	A12_G_35	A17_G_35	A21_G_35	A24_G_35
RH=75 %	Standard	A12_S_75	A17_S_75	A21_S_75	A24_S_75
	Machined	A12_M_75	A17_M_75	A21_M_75	A24_M_75
	Greased	A12_G_75	A17_G_75	A21_G_75	A24_G_75
RH=95 %	Standard	A12_S_95	A17_S_95	A21_S_95	A24_S_95
	Machined	A12_M_95	A17_M_95	A21_M_95	A24_M_95
	Greased	A12_G_95	A17_G_95	A21_G_95	A24_G_95

Table 7-2. Full test matrix for the specimens prepared with 50 MPa compaction pressure.

Compaction pressure: 50 MPa					
Water content		**as-delivered**	**17 %**	**21 %**	**24 %**
RH=35 %	Standard	B12_S_35	B17_S_35	B21_S_35	B24_S_35
	Machined	B12_M_35	B17_M_35	B21_M_35	B24_M_35
	Greased	B12_G_35	B17_G_35	B21_G_35	B24_G_35
RH=75 %	Standard	B12_S_75	B17_S_75	B21_S_75	B24_S_75
	Machined	B12_M_75	B17_M_75	B21_M_75	B24_M_75
	Greased	B12_G_75	B17_G_75	B21_G_75	B24_G_75
RH=95 %	Standard	B12_S_95	B17_S_95	B21_S_95	B24_S_95
	Machined	B12_M_95	B17_M_95	B21_M_95	B24_M_95
	Greased	B12_G_95	B17_G_95	B21_G_95	B24_G_95

7.4 Results

7.4.1 Relative Humidity equilibrium

The water retention curve is a relation between the water content and the energy state or potential of the soil water expressed as relative humidity or suction.

Bentonite material with four different water contents has been used in this investigation. For each of the water contents, the relative humidity at equilibrium has been measured. The bentonite specimens were placed in special jars with tight lids where it was possible to continuously register the relative humidity just above the bentonite surface. After having finished the measurement, the water content of the bentonite was determined. Measurements were made with both bentonite powder and with compacted specimens. The determined data is provided in Table 7-3 and in Figure 7-4. The determined relative humidity equilibrium is somewhat lower for the compacted specimens compared to the powder with the same water content. The variation in results may depend on very small differences in water content locally over the surface of the compacted samples i.e. if the bentonite is taking up water or if it is drying (absorption or desorption), see Figure 7-17.

Table 7-3. Determined Relative Humidity at equilibrium for different water contents for both powder and block

Sample	Water content %	RH %
Powder	10.55	50.6
Powder	16.69	73.3
Powder	20.76	85.3
Powder	23.66	91.3
Block	10.57	49.1
Block	16.71	70.1
Block	20.71	81.7
Block	23.70	89.9

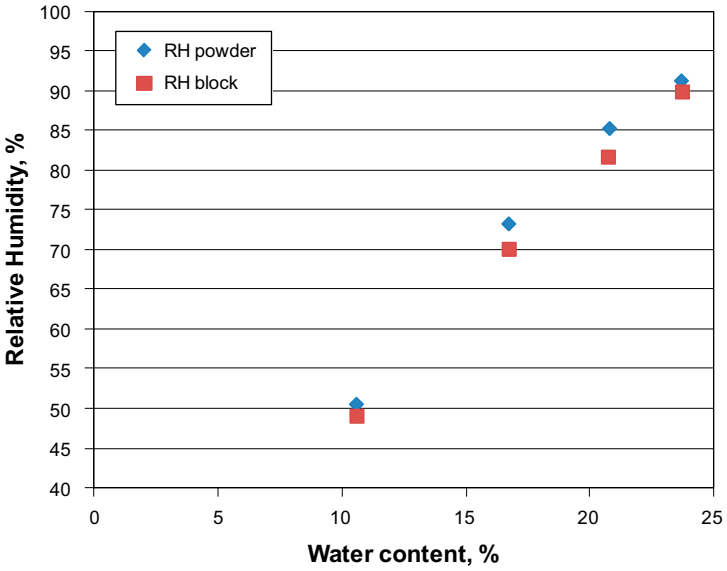

Figure 7-4. Graph showing the measured Relative Humidity plotted versus the water content of the material.

7.4.2 The effect of exposure to different Relative Humidities

As described the specimens were placed in the climate chamber, after weighing and dimension measurements. After 2 hours they were again weighed and a photo was taken with observations of any cracks etc. This was repeated with increasing interval until the test was finished. After each weighing the change in mass, expressed as mass difference from initial value, was calculated. The results are presented in the following diagram, where the mass difference is on the y axis (in %) versus the time (in hours). After test termination, the dimensions were measured again and the water content and density for each specimen was determined. In Appendix 13 the photos of each test at the start and end are collected and all measured data is provided in Appendix 14. Detailed photos of significant details are presented together with the results.

Results 35 % Rh

The results from the specimens placed in a climate chamber with a relative humidity of 35 % are provided in Figure 7-5 (specimens compacted with 25 MPa) and 7-6 (specimens compacted with 50 MPa). Some specimens in this climate, 35 % Rh, showed small radial cracks after only two hours, these were gone again after 24–48 hours, see example provided in Figure 7-7. This was only apparent on the specimens with an initial water content of 21 % and 24 %.

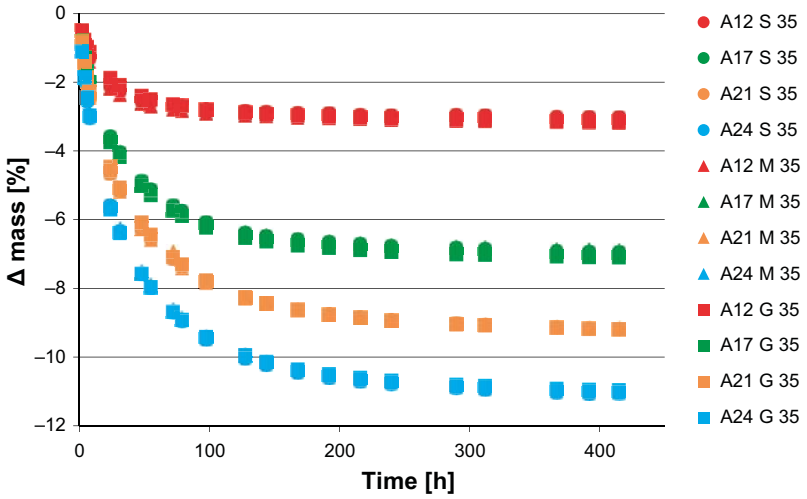

Figure 7-5. *Changes in mass for specimens compacted at 25 MPa in 35 % Rh environment. The designations of the specimens are described in Table 7-1.*

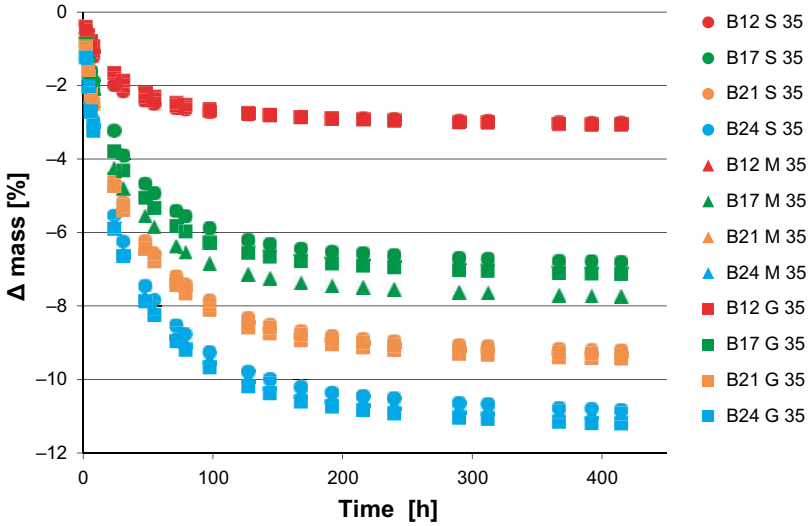

Figure 7-6. *Changes in mass for specimens compacted at 50 MPa in 35 % Rh environment. The designations of the specimens are described in Table 7-2.*

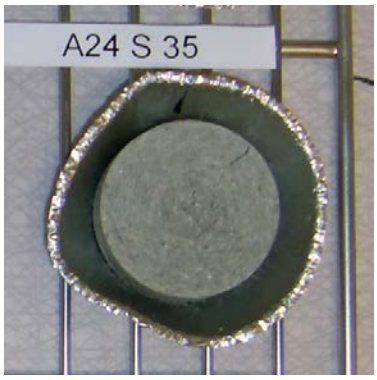

Figure 7-7. *Photo of specimen A24 M 35 with small radial crack at 45° (0° straight up), this later "healed" after approximately 48 hours.*

All specimens' lost weight when exposed to this relative humidity. The volumetric change of each specimen was almost the same as the volume of the lost water for these specimens. The determined water content after test termination varied between 7.1 to 8.8 %, see data provided in Appendix 14.

Result 75 % Rh

The results from the specimens placed in a climate chamber with a relative humidity of 75 % are provided in Figure 7-8 (specimens compacted with 25 MPa) and 7-9 (specimens compacted with 50 MPa). Three of the specimens (12 % initial water content) have increased their weight; three specimens' shows almost no difference in weight (17 % initial water content) while the rest of the specimens have lost weight when exposed to this relative humidity (21 and 24 % initial water content). The determined water content after test termination varied between 14.7 to 19 %, see data provided in Appendix 14.

In this relative humidity most specimens showed small changes in weight and only two specimens had by eye visible changes. One machined specimen A12 M 75 that had a "crust" that started to separate, see Figure 7-10 and also specimen B12 S 75 where small radial cracks started to develop after 8 hours and later healed after three days exposure.

The volumetric change was almost the same as the mass change except for the specimens with low initial water content that were expanding more in volume than mass.

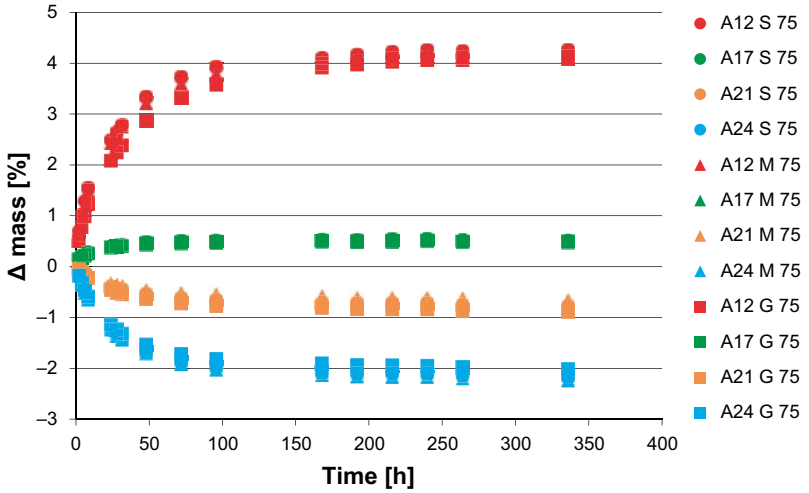

Figure 7-8. *Changes in mass for specimens compacted at 25 MPa in 75 % Rh environment. The designations of the specimens are described in Table 7-1.*

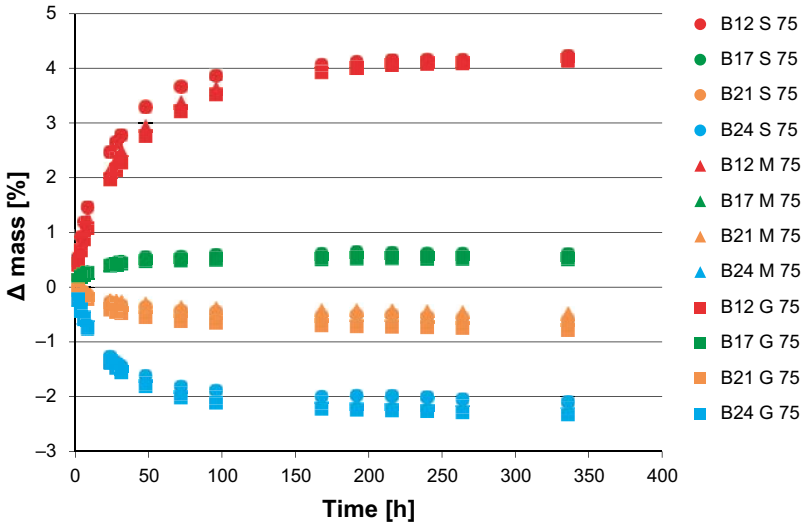

Figure 7-9. *Changes in mass for specimens compacted at 50 MPa in 75 % Rh environment. The designations of the specimens are described in Table 7-2.*

Figure 7-10. *Photo of A12 M 75 where the top surface started to peel off.*

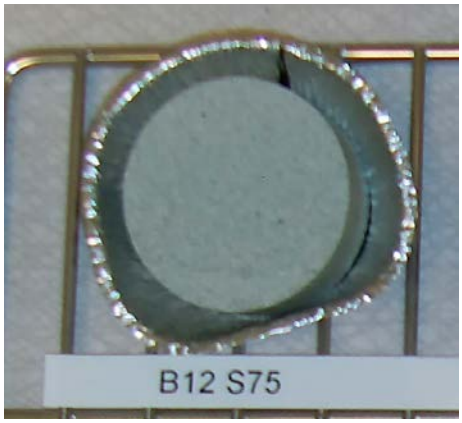

Figure 7-11. *Fine cracks at 180°–270°, hardly visible, healed after 72 h.*

Result 95 % Rh

The results from the specimens placed in a climate chamber with a relative humidity of 95 % are provided in Figure 7-12 (specimens compacted with 25 MPa) and 7-13 (specimens compacted with 50 MPa). In this relative humidity all specimens with an initial water content of 12 % reacted within 2 hours and showed circular cracks that didn't heal, see Figure 7-14 and 7-15.

All specimens' increased their weight when exposed to this relative humidity. The determined water content after test termination varied between 22.8 to 24.6 %, see data provided in Appendix 14.

The specimens with an initial water content of 12 % could not be divided into two parts after the test but crumbled when handled. The volume expansion was also significantly higher than mass change. Due to the cracking, the volumetric change of each specimen was large.

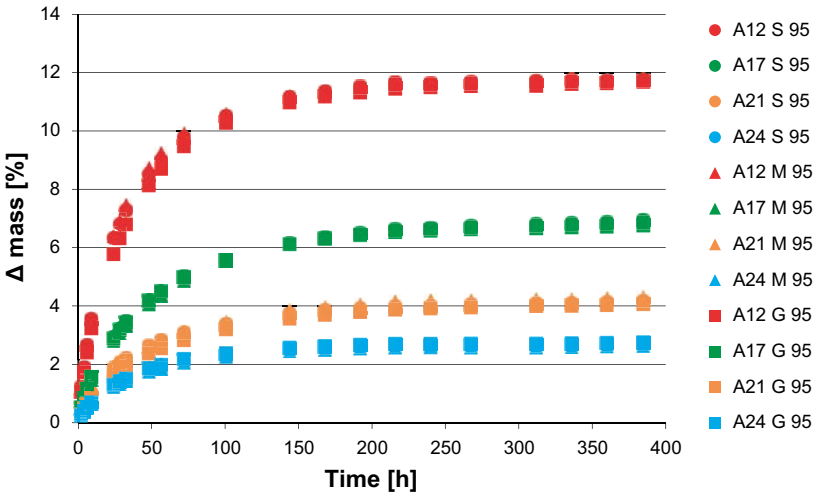

Figure 7-12. *Changes in mass for specimens compacted at 25 MPa in 95 % Rh environment. The designations of the specimens are described in Table 7-1.*

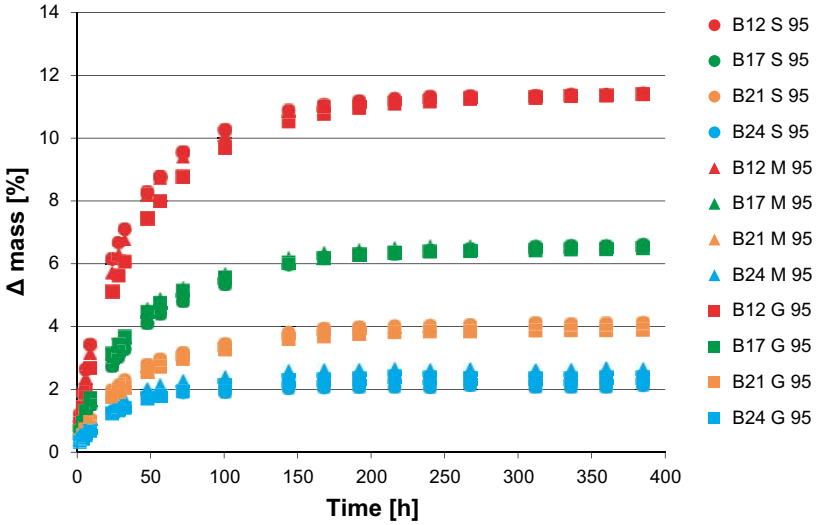

Figure 7-13. *Changes in mass for specimens compacted at 50 MPa in 95 % Rh environment. The designations of the specimens are described in Table 7-2.*

Figure 7-14. *Circular cracks in A12 S 95 after 2 hours.*

Figure 7-15. *Cracks in A12 M 95 after 168 hours.*

An example of the water uptake behavior for three identical specimens with an initial water content of 17 % when exposed to three different relative humidities is shown in Figure 7-16.

In Figure 7-17 the final water contents for each specimen, is plotted as a function of the relative humidity that they have been exposed to. The graph also shows the relative humidity equilibrium for the start material i.e. the same as was shown in Figure 7-4. The black dotted lines show the retention curves determined by Dueck and Nilsson (2010). The upper line represents desorption and the lower absorption. As shown in the graph, all specimens that have been placed in 35 % have dried somewhat and that is why they are closer to the desorption line while the specimens that were placed in 95 % relative humidity have taken up water and are therefore closer to the absorption line. The specimens placed in 75 % relative humidity have both taken up water (initial water content of 12 %) and dried (initial water content of 24 %) and this is the explanation for the large spread in determined water content after test.

As shown in the graph, there is an evident distribution regarding the final water content for all specimens exposed to a certain relative humidity i.e. all specimens do not reach exactly the same water content after equilibrium. This distribution depends largely on the water content at start of the single specimen. The graph provided in Figure 7-18, shows the final water content for the three different relative humidities plotted versus the water content at start for all specimens. The graph shows that the distribution in results regarding the final water content after equilibrium at a certain relative humidity mainly depends on the water content at start i.e. there is a hysteresis in the bentonite material. High initial water content will result in somewhat higher water content also after equilibrium at a certain relative humidity.

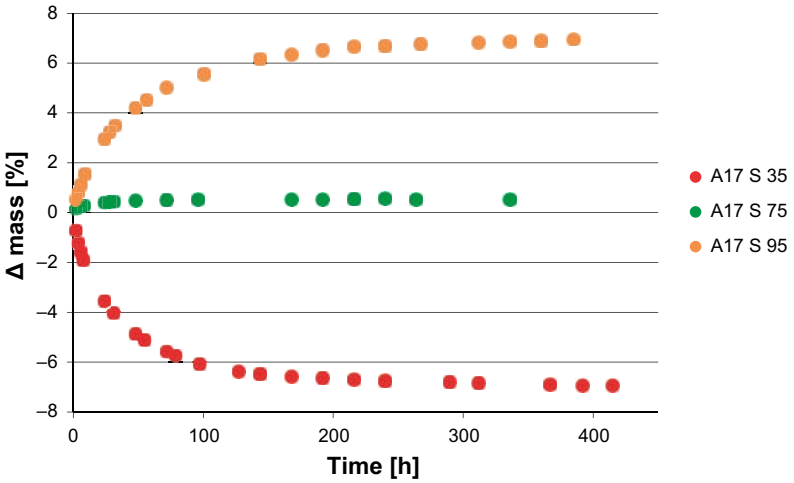

Figure 7-16. *Mass change for the A17 specimen in different Rh (35, 75 and 95 %). The designations of the specimens are described in Table 7-1.*

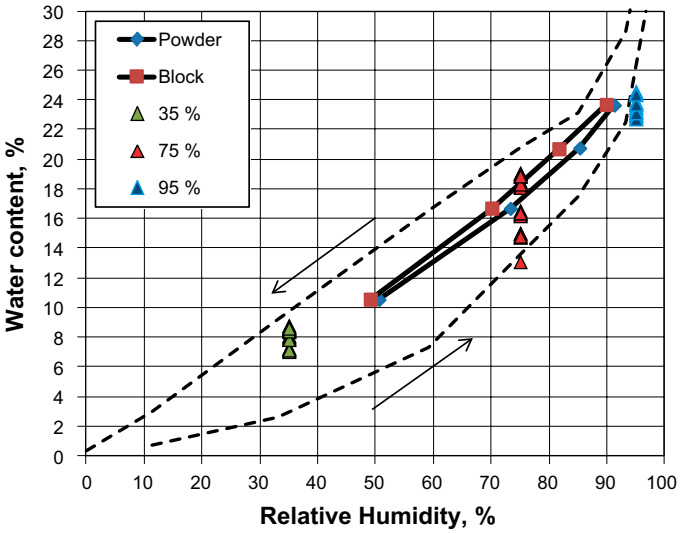

Figure 7-17. *Final water content for all specimens plotted as a function of the relative humidity they have been exposed to. The graph also shows the relative humidity equilibrium for the start material. The black dotted lines show the retention curves determined by Dueck and Nilsson (2010).*

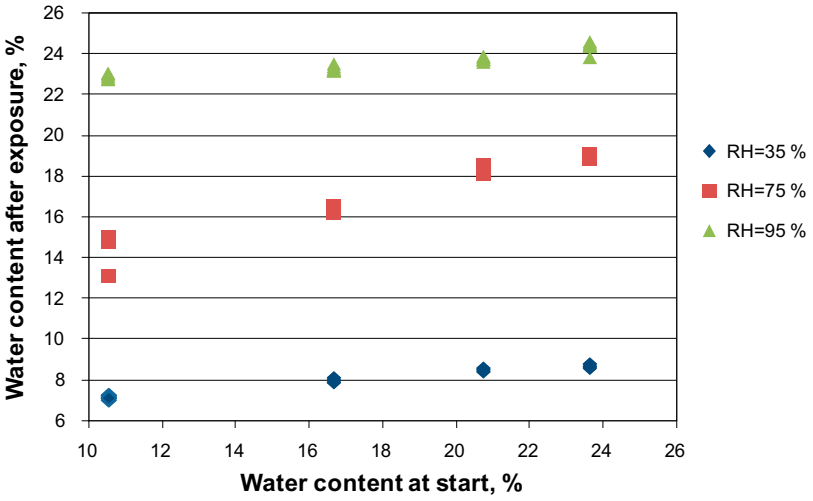

Figure 7-18. *Water content after exposure plotted versus the water content at test start.*

7.5 Comments and conclusions

From the performed tests the following comments and conclusions have been made:

- There was no evident influence of previous treatment (standard, machined or greased) regarding the water uptake detected during the test time.
- Independent of the initial water content, the specimens had stabilized after 100–200 hours with most mass changes taking place the first 100 hours, in all three relative humidities.
- Specimens with an initial water content of 21 % and 24 % achieved some small cracks when exposed to 35 % relative humidity. The cracks had, however, healed after 24–48 hours. No remaining cracks were detected in blocks with initial water contents >17 %.
- Specimens with an initial water content of 12 % cracked and were structural instable at the end of the test when exposed to 95 % relative humidity. The effect was more pronounced for the specimens with machined surfaces.
- There were small differences between the specimens compacted at 25 or 50 MPa.

8 Summary and conclusions

8.1 General

This report describes laboratory investigations made in order to study how different material parameters influence the achieved backfill block quality. In addition an investigation aiming to study the influence of different relative humidity on the backfill blocks has been performed. The following have been investigated and/or determined:

- Granule size distribution of the raw material used for block compaction.
- Determination of the grain density.
- Determination of the density of individual granules
- Determination of the tensile strength of backfill blocks and how the strength is influenced of granule size distribution, water content and density (void ratio).
- Relative humidity induced cracking on backfill blocks.

8.2 Granule size distribution

Earlier tests have shown that the achieved block quality seems to be depending on the granule size distribution of the raw material. In the performed tests the as-delivered bentonite has been used together with milled bentonite and bentonite where the fines (<1mm) have been removed by sieving. The granule size distribution of the different materials (as-delivered and produced) has then been determined. In the performed tests, the following bentonites have been used:

- MX-80 from Wyoming USA, batches from 2002 and 2012.
- SPV200 from Wyoming USA, old batch from storage (Clay Technology AB).
- Ibeco RWC-BF, batch from 2011.
- Asha NW BFL-L, batches from 2010 and 2012.

After determination of the granule size distribution the different bentonite materials have been used to compact specimens for the block strength tests.

8.3 Grain density

The grain density of the Asha materials was as expected significant higher than the other materials. The high grain density of these materials is attributed to the high iron content. The average grain density for Asha 2010 was determined to 2888 kg/m^3 and for Asha 2012 to 2912 kg/m^3. The grain density for Ibeco 2011 was determined to 2806 kg/m^3 which is somewhat higher than in earlier investigations with this material. The determined average grain density of material from the two MX-80 batches was almost the same, between 2802 and 2809 kg/m^3. The grain density of the SPV200 material was considerably lower with an average of 2658 kg/m^3. This indicates that the origin of this material is not the same as the MX-80.

8.4 Granule density

The density of the individual granules was determined for four materials:

- Asha 2010 batch. The granules are angular and seem to be very hard. The average granule dry density was found to be 1764 kg/m^3.
- Asha 2012. The granules are flat and seem to be somewhat softer than the ones from 2010. The average granule dry density was found to be 1786 kg/m^3.

- Ibeco 2011. The granules are smaller and rather soft. The average granule dry density was found to be 1618 kg/m^3.
- MX-80. In this test the granules from crushed pellets were tested. The granules are angular and seem to be rather stiff. The average granule dry density was found to be 1820 kg/m^3.

8.5 Block strength

From the performed tests it was concluded that the three parameters investigated, granule size distribution, dry density (void ratio) and water content are all strongly influencing the achieved block strength.

The tested materials have large differences in density of the solids. This means that if one wants to study the influence of the void volume relative the volume of the solids on the achieved tensile strength, the tensile strength should be plotted versus the void ratio. E.g. when comparing MX-80 and Asha (density of solids of 2800 and 2910 kg/m^3 respectively) for a block dry density of 1700 kg/m^3 the difference in void ratio is approximately 10 %.

During the performance of the beam tests it was discovered that a few specimens were rather brittle and it was not possible to saw out beams of good quality. This problem occurred for Asha and Ibeco specimens with the lowest water content and with large granules. This indicates that the raw material should not be too coarse. The beam tests show that it is favourable to crush the materials in order to increase the block strength at least at higher void ratios. The achieved strength of the crushed material seems to be less dependent of the water content than the uncrushed materials. However, in order to facilitate the handling of the bulk material e.g. regarding dust, it is probably favourable to increase the water content somewhat.

8.6 Relative humidity induced cracking

The performed tests where compacted specimens were exposed to different relative humidity showed that there was no evident influence of previous treatment of the exposed surfaces (standard, machined or greased) regarding the water uptake detected during the test time.

The initial water content of the specimens is, however, an important factor for the behavior when exposed to different relative humidity. Specimens with an initial water content of 21 % and 24 % achieved some small cracks when exposed to 35 % relative humidity and specimens with an initial water content of 12 % cracked and were structural instable at the end of the test when exposed to 95 % relative humidity.

Installation of bentonite blocks in a deposition tunnel will be facilitated if extreme relative humidities can be avoided. The relative humidity will probably be rather high i.e. >75 % (depending on ventilation, time of the year etc.) and in tunnels where the ventilation system has been removed e.g. due to the installation process, the relative humidity can be above 90 %. Bentonite blocks with water contents between 17 and 22 %, will be more stable during these conditions which will facilitate the block handling.

8.7 Recommendations and further work

The performed tests show that there are still uncertainties regarding the influence of granule size distribution on the achieved block strength. An additional minor study is planned where the material will be sieved into different fractions before compaction to block and a following strength test.

The performed tests give, however, some indications regarding processing of the raw material for manufacturing of backfill blocks:

1. The block strength tests indicate that it is favorable to crush the raw material somewhat especially if it contains large granules; > 5mm. The maximum granule size should probably be somewhere between 1 and 2 mm.

2. High water content increases the block strength and improves the block behavior when exposed to different relative humidities (less prone for cracking). The optimal water content is probably between 17 and 22 %.

It should however be mentioned that it always will be necessary to perform tests when introducing a new material before starting up production in large scale. This is the most common way to handle new material e.g. within the industry manufacturing refractory bricks.

Access to different equipment for material processing (e.g. crushers, sieves and mixers) will facilitate the large scale production and will also give the possibility to handle raw materials with different properties.

References

SKB's (Svensk Kärnbränslehantering AB) publications can be found at www.skb.se/publications.

Dueck A, Nilsson U, 2010. Thermo-hydro-mechanical properties of MX-80. Results from advanced laboratory tests. SKB TR-10-55, Svensk Kärnbränslehantering AB.

Sandén T, Olsson S, Andersson L, Dueck A, Jensen V, Hansen E, Johnsson A, 2014. Investigation of backfill candidate materials. SKB R-13-08, Svensk Kärnbränslehantering AB.

Sandén T, Andersson L, Jensen V, 2015. System design of backfill. Full scale production test of backfill blocks. SKB P-14-24, Svensk Kärnbränslehantering AB.

Karnland O, Olsson S, Nilsson U, 2006. Mineralogy and sealing properties of various bentonites and smectite-rich clay materials. SKB TR-06-30, Svensk Kärnbränslehantering AB.

Appendix 1

Photos of specimens after compaction, test series 1, ASHA

Appendix 2

Photos of specimens after compaction, test series 1, IBECO

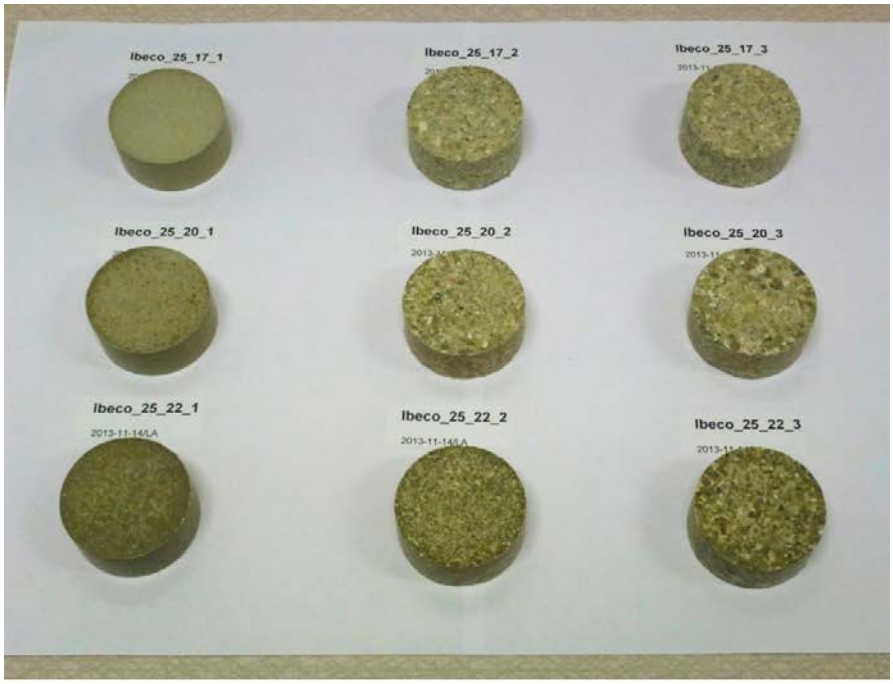

Appendix 3

Photos of specimens after compaction, test series 1, MX-80

Appendix 4

Photos of specimens after compaction, test series 2, ASHA

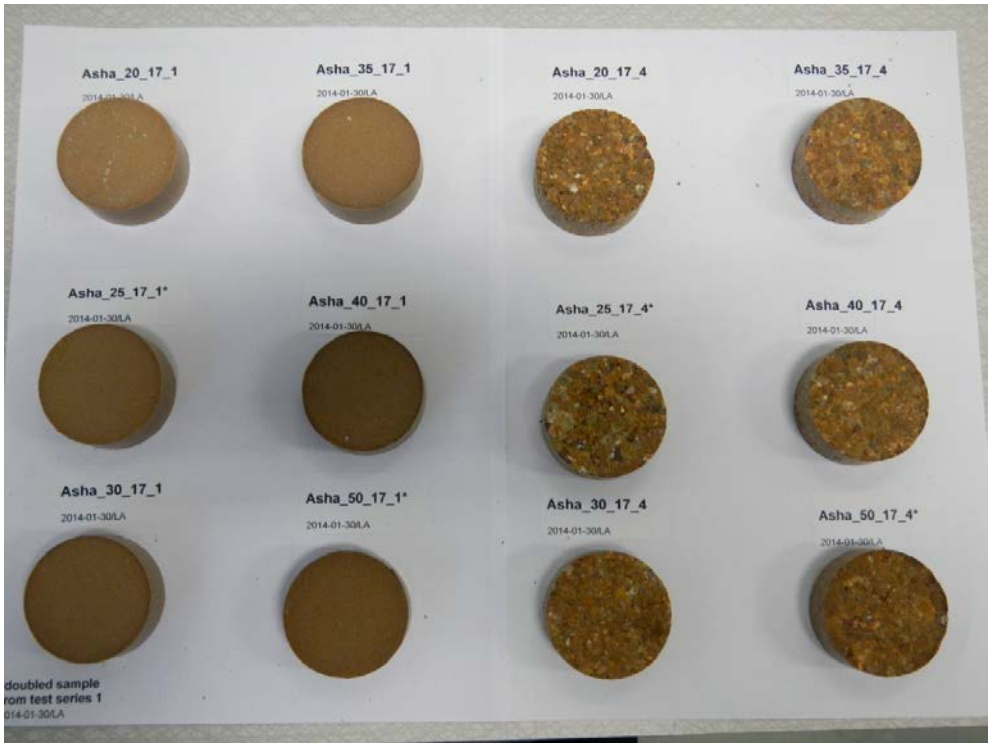

Appendix 5

Photos of beams after sawing, test series 1, ASHA

Appendix 6

Photos of beams after sawing, test series 1, IBECO

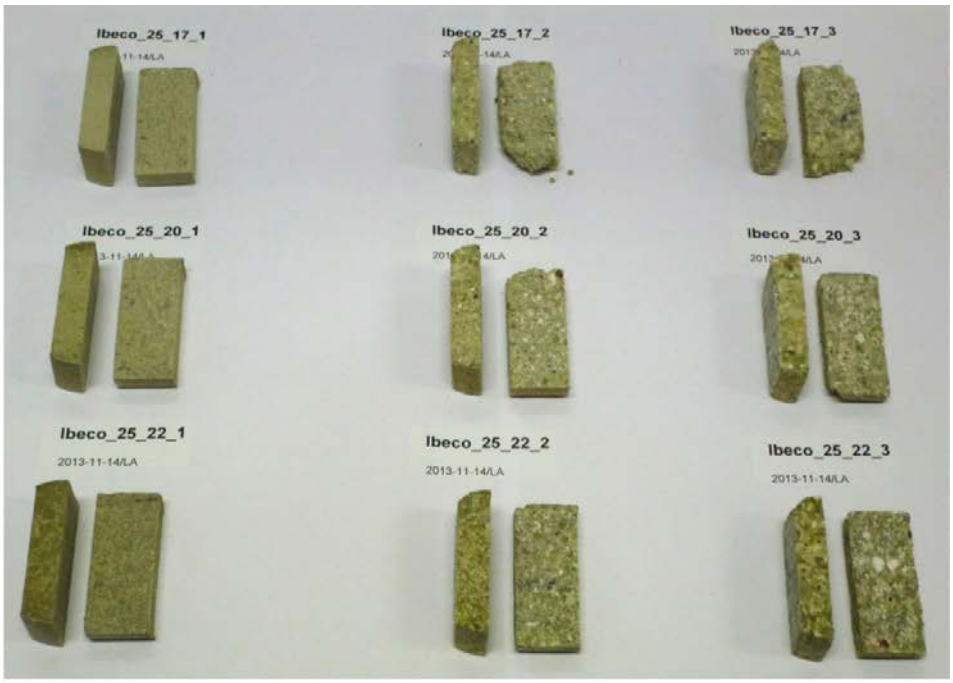

Appendix 7

Photos of beams after sawing, test series 1, MX-80

Appendix 8

Photos of beams after sawing, test series 2, ASHA

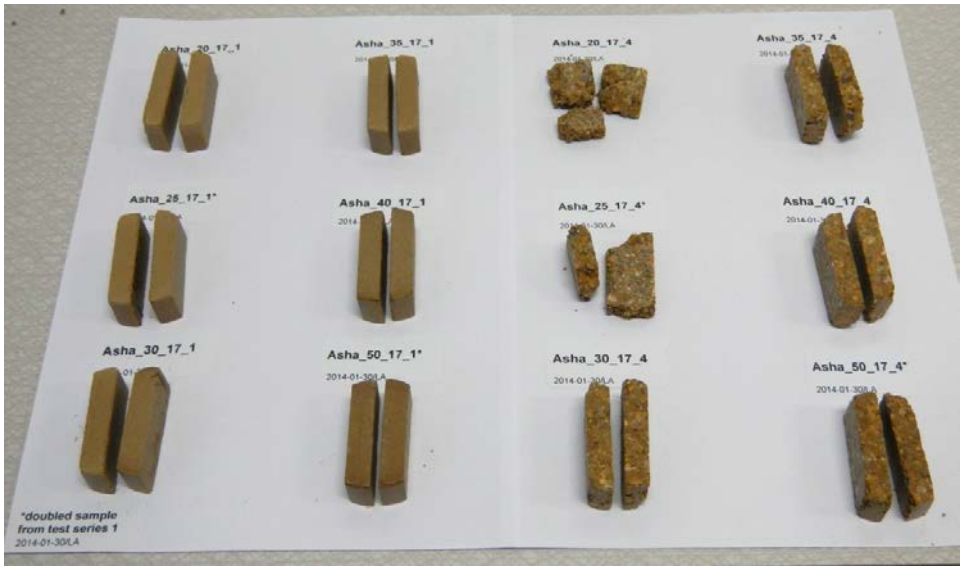

Appendix 9

Photos of beams after sawing, test series 2, MX-80

Appendix 10

Table showing all data from beam tests, IBECO

Test ID	Comp. Pressure MPa	Water content %	Dry density kg/m^3	Void ratio	Strain at failure %	Max. tensile stress kPa
IBECO_25_17_1A	25	15.7	1772	0.584	0.779	1067
IBECO_25_17_1B	25	15.7	1772	0.584	0.713	1105
IBECO_25_20_1A	25	18.0	1788	0.569	0.786	1179
IBECO_25_20_1B	25	18.0	1788	0.569	0.639	1158
IBECO_25_22_1A	25	19.8	1769	0.586	1.206	1390
IBECO_25_22_1B	25	19.8	1769	0.586	1.307	1636
IBECO_25_17_2A	25	15.0	1757	0.597	0.956	836
IBECO_25_17_2B	25	15.0	1757	0.597	0.962	556
IBECO_25_20_2A	25	17.3	1730	0.622	0.754	1242
IBECO_25_20_2B	25	17.3	1730	0.622	0.87	1506
IBECO_25_22_2A	25	18.8	1753	0.601	0.957	1545
IBECO_25_22_2B	25	18.8	1753	0.601	1.165	1027
IBECO_25_17_3A	25	14.6	1732	0.620	0.889	245
IBECO_25_17_3B	25	14.6	1732	0.620	1.091	219
IBECO_25_20_3A	25	16.7	1749	0.604	1.176	776
IBECO_25_20_3B	25	16.7	1749	0.604	0.946	718
IBECO_25_22_3A	25	18.2	1763	0.592	0.801	1014
IBECO_25_22_3B	25	18.2	1763	0.592	1.018	1024
IBECO_50_17_1A	50	15.8	1856	0.512	0.634	2604
IBECO_50_17_1B	50	15.8	1856	0.512	0.564	1279
IBECO_50_20_1A	50	17.9	1831	0.532	0.858	1938
IBECO_50_20_1B	50	17.9	1831	0.532	0.905	1115
IBECO_50_22_1A	50	19.5	1795	0.563	1.247	1332
IBECO_50_22_1B	50	19.5	1795	0.563	1.339	1358
IBECO_50_17_2A	50	14.6	1833	0.531	0.838	1219
IBECO_50_17_2B	50	14.6	1833	0.531	0.902	1256
IBECO_50_20_2A	50	17.5	1822	0.540	1.097	1927
IBECO_50_20_2B	50	17.5	1822	0.540	0.921	1258
IBECO_50_22_2A	50	19.0	1792	0.566	1.046	1566
IBECO_50_22_2B	50	19.0	1792	0.566	0.995	1578
IBECO_50_17_3A	50	15.5	1800	0.559	0.753	739
IBECO_50_17_3B	50	15.5	1800	0.559	0.764	784
IBECO_50_20_3A	50	18.0	1785	0.572	0.936	1290
IBECO_50_20_3B	50	18.0	1785	0.572	0.55	1064
IBECO_50_22_3A	50	19.4	1746	0.607	0.802	1433
IBECO_50_22_3B	50	19.4	1746	0.607	0.932	895

Appendix 11

Table showing all data from beam tests, MX-80

Test ID	Comp. Pressure MPa	Water content %	Dry density kg/m³	Void ratio	Strain at failure %	Max. tensile stress kPa
MX-80_25_12_1A	25	9.4	1617	0.644	1.072	940
MX-80_25_12_1B	25	9.4	1617	0.644	0.921	1141
MX-80_25_17_1A	25	17.0	1647	0.614	0.716	1187
MX-80_25_17_1B	25	17.0	1647	0.614	0.512	1020
MX-80_25_21_1A	25	20.1	1671	0.591	0.852	1570
MX-80_25_21_1B	25	20.1	1671	0.591	0.694	1120
MX-80_25_12_2A	25	8.7	1651	0.690	0.449	216
MX-80_25_12_2B	25	8.7	1651	0.690	0.558	193
MX-80_25_17_2A	25	16.0	1661	0.680	0.79	1123
MX-80_25_17_2B	25	16.0	1661	0.680	0.803	1026
MX-80_25_21_2A	25	18.3	1679	0.662	0.542	854
MX-80_25_21_2B	25	18.3	1679	0.662	0.872	1263
MX-80_25_12_3A	25	10.2	1707	0.634	0.656	1209
MX-80_25_12_3B	25	10.2	1707	0.634	0.622	968
MX-80_25_17_3A	25	16.4	1709	0.633	0.628	1542
MX-80_25_17_3B	25	16.4	1709	0.633	0.607	1121
MX-80_25_21_3A	25	18.5	1713	0.629	0.726	1835
MX-80_25_21_3B	25	18.5	1713	0.629	0.605	1217
MX-80_25_12_4A	25	12.8	1808	0.543	0.584	689
MX-80_25_12_4B	25	12.8	1808	0.543	0.721	580
MX-80_25_17_4A	25	16.3	1748	0.596	0.44	1033
MX-80_25_17_4B	25	16.3	1748	0.596	0.824	895
MX-80_25_21_4A	25	19.9	1726	0.616	0.792	1037
MX-80_25_21_4B	25	19.9	1726	0.616	0.84	1397
MX-80_50_12_1A	50	9.4	1762	0.509	0.653	2069
MX-80_50_12_1B	50	9.4	1762	0.509	0.661	1756
MX-80_50_17_1A	50	16.7	1750	0.519	0.559	1760
MX-80_50_17_1B	50	16.7	1750	0.519	0.693	1709
MX-80_50_21_1A	50	20.1	1738	0.529	0.831	1462
MX-80_50_21_1B	50	20.1	1738	0.529	0.759	1858
MX-80_50_12_2A	50	8.7	1790	0.559	0.73	1336
MX-80_50_12_2B	50	8.7	1790	0.559	0.683	1301
MX-80_50_17_2A	50	15.9	1755	0.590	0.632	1781
MX-80_50_17_2B	50	15.9	1755	0.590	0.501	1755
MX-80_50_21_2A	50	18.7	1752	0.592	0.602	2238
MX-80_50_21_2B	50	18.7	1752	0.592	0.769	1756
MX-80_50_12_3A	50	10.4	1850	0.508	0.539	2669
MX-80_50_12_3B	50	10.4	1850	0.508	0.66	2485
MX-80_50_17_3A	50	16.8	1785	0.563	0.733	1936
MX-80_50_17_3B	50	16.8	1785	0.563	0.817	1892
MX-80_50_21_3A	50	19.1	1772	0.574	0.777	1988
MX-80_50_21_3B	50	19.1	1772	0.574	0.801	1818
MX-80_50_12_4A	50	12.8	1883	0.482	0.549	1675
MX-80_50_12_4B	50	12.8	1883	0.482	0.569	1896
MX-80_50_17_4A	50	16.3	1803	0.547	0.762	1798
MX-80_50_17_4B	50	16.3	1803	0.547	0.614	1861
MX-80_50_21_4A	50	20.2	1751	0.593	0.673	1884
MX-80_50_21_4B	50	20.2	1751	0.593	1.04	1244

Appendix 12

Table showing all data from beam tests, Test series II (ASHA and MX-80)

Test ID	Comp. Pressure MPa	Water content %	Dry density kg/m³	Void ratio	Strain at failure %	Max. tensile stress kPa
ASHA_20_17_1A	20	16.51	1684	0.722	0.589	831
ASHA_20_17_1B	20	16.51	1684	0.722	0.458	783
ASHA_25_17_1A*	25	16.58	1738	0.669	0.562	1029
ASHA_25_17_1B*	25	16.58	1738	0.669	0.529	1073
ASHA_30_17_1A	30	16.67	1766	0.642	0.661	1151
ASHA_30_17_1B	30	16.67	1766	0.642	0.528	1577
ASHA_35_17_1A	35	16.67	1792	0.618	0.597	2182
ASHA_35_17_1B	35	16.67	1792	0.618	0.582	1339
ASHA_40_17_1A	40	16.67	1811	0.601	0.519	1759
ASHA_40_17_1B	40	16.67	1811	0.601	0.76	1249
ASHA_50_17_1A*	50	16.57	1842	0.574	0.503	1319
ASHA_50_17_1B*	50	16.57	1842	0.574	0.631	1319
ASHA_20_17_4A	20	16.97	1702	0.704		
ASHA_20_17_4B	20	16.97	1702	0.704		
ASHA_25_17_4A*	25	16.59	1709	0.697	0.543	134
ASHA_25_17_4B*	25	16.59	1709	0.697		
ASHA_30_17_4A	30	17	1737	0.670	0.658	257
ASHA_30_17_4B	30	17	1737	0.670	0.716	259
ASHA_35_17_4A	35	16.72	1757	0.651	0.606	370
ASHA_35_17_4B	35	16.72	1757	0.651	0.684	325
ASHA_40_17_4A	40	16.84	1767	0.641	0.461	326
ASHA_40_17_4B	40	16.84	1767	0.641	0.509	539
ASHA_50_17_4A*	50	16.61	1802	0.609	0.613	646
ASHA_50_17_4B*	50	16.61	1802	0.609	0.54	606
MX-80_20_17_1A	20	17.86	1617	0.644	0.6	1117
MX-80_20_17_1B	20	17.86	1617	0.644	0.473	822
MX-80_25_17_1A*	25	17.85	1674	0.588	0.697	1011
MX-80_25_17_1B*	25	17.85	1674	0.588	0.631	1212
MX-80_30_17_1A	30	17.73	1694	0.569	0.598	1445
MX-80_30_17_1B	30	17.73	1694	0.569	0.651	1338
MX-80_35_17_1A	35	17.79	1714	0.551	0.72	1377
MX-80_35_17_1B	35	17.79	1714	0.551	0.545	1384
MX-80_40_17_1A	40	17.94	1721	0.544	0.711	1184
MX-80_40_17_1B	40	17.94	1721	0.544	0.593	1234
MX-80_50_17_1A*	50	17.89	1749	0.520	0.503	1367
MX-80_50_17_1B*	50	17.89	1749	0.520	0.615	1607
MX-80_20_17_4A	20	16.03	1737	0.606	0.58	855
MX-80_20_17_4B	20	16.03	1737	0.606	0.611	950
MX-80_25_17_4A*	25	15.96	1759	0.586	0.511	1123
MX-80_25_17_4B*	25	15.96	1759	0.586	0.769	871
MX-80_30_17_4A	30	15.93	1790	0.559	0.62	1097
MX-80_30_17_4B	30	15.93	1790	0.559	0.507	1096
MX-80_35_17_4A	35	16.03	1796	0.553	0.602	957
MX-80_35_17_4B	35	16.03	1796	0.553	0.647	1128
MX-80_40_17_4A	40	16.02	1800	0.550	0.626	1429
MX-80_40_17_4B	40	16.02	1800	0.550	0.735	1362
MX-80_50_17_4A*	50	16.04	1811	0.541	0.583	1514
MX-80_50_17_4B*	50	16.04	1811	0.541	0.858	1442

Appendix 13

Photos of the specimens before and after the test

A13-1. *The A specimens before the 35 % Rh test.*

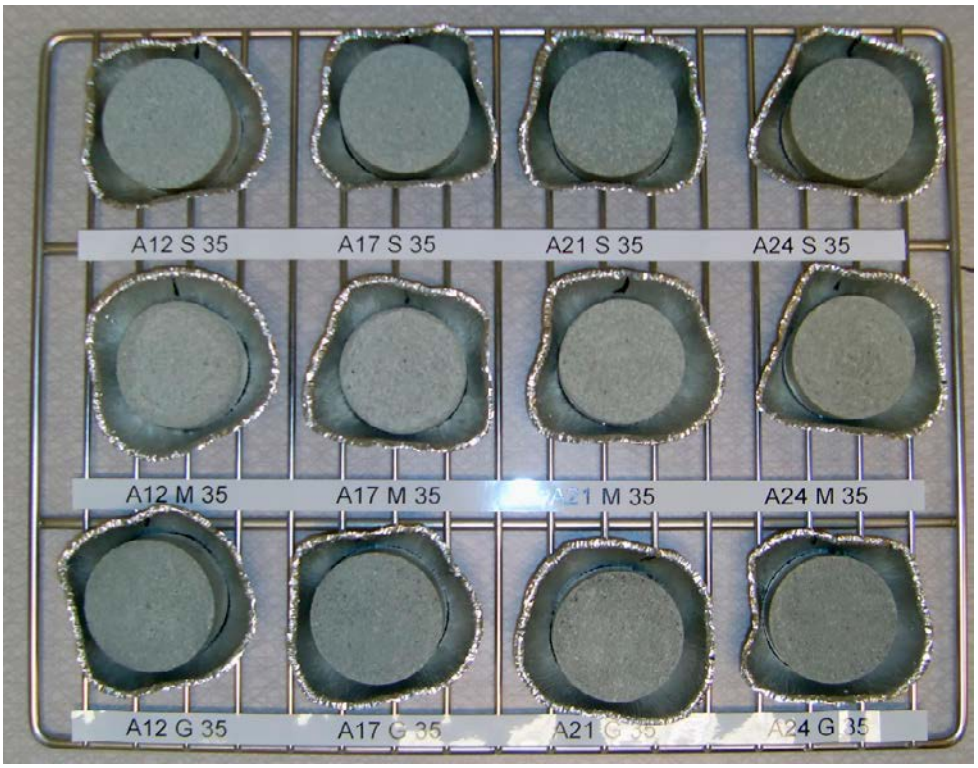

A13-2. *The A specimens after the 35 % Rh test.*

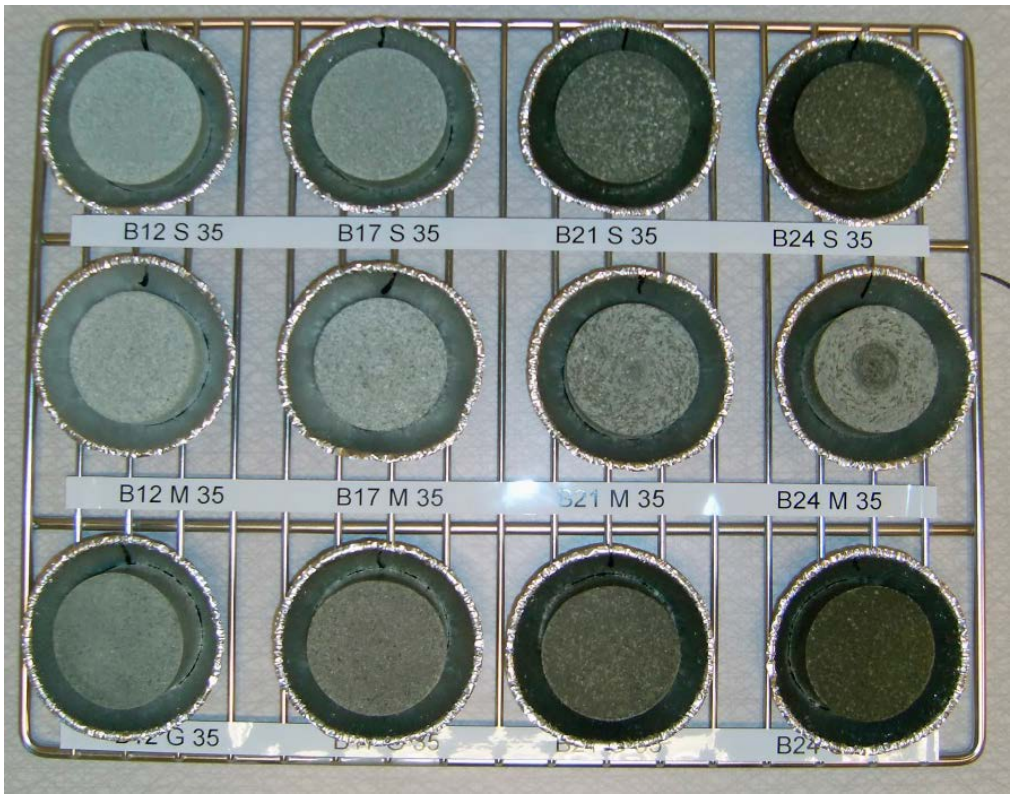

A13-3. *The B specimens before the 35 % Rh test.*

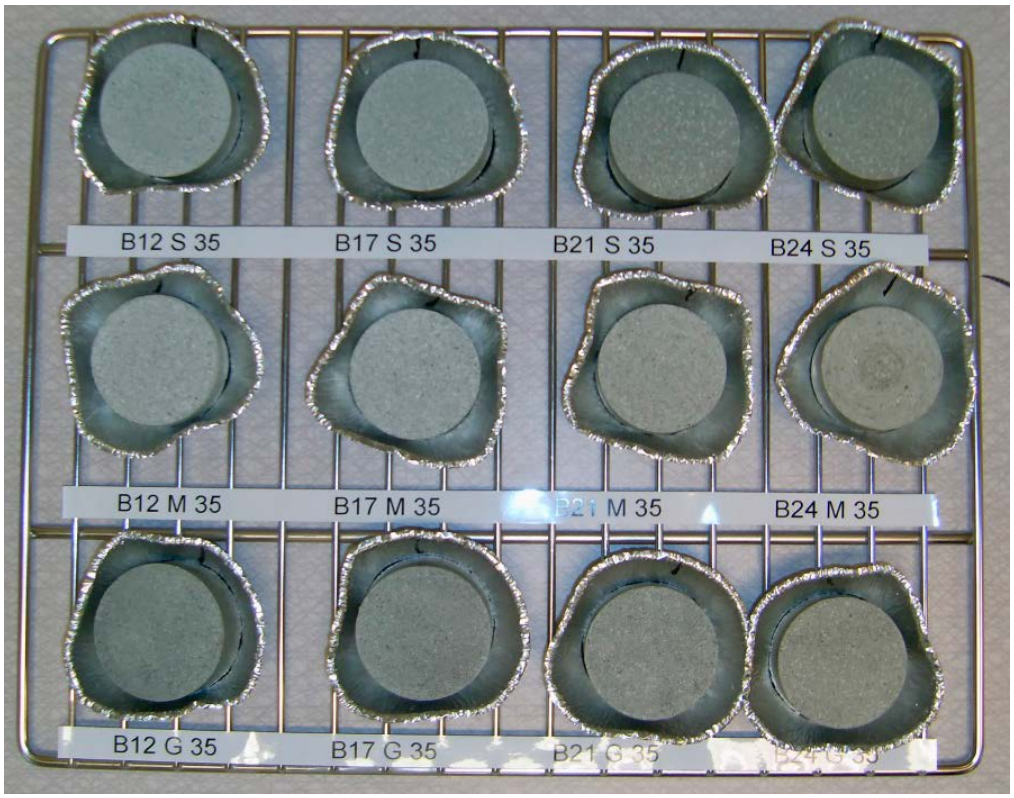

A13-4. *The B specimens after the 35 % Rh test.*

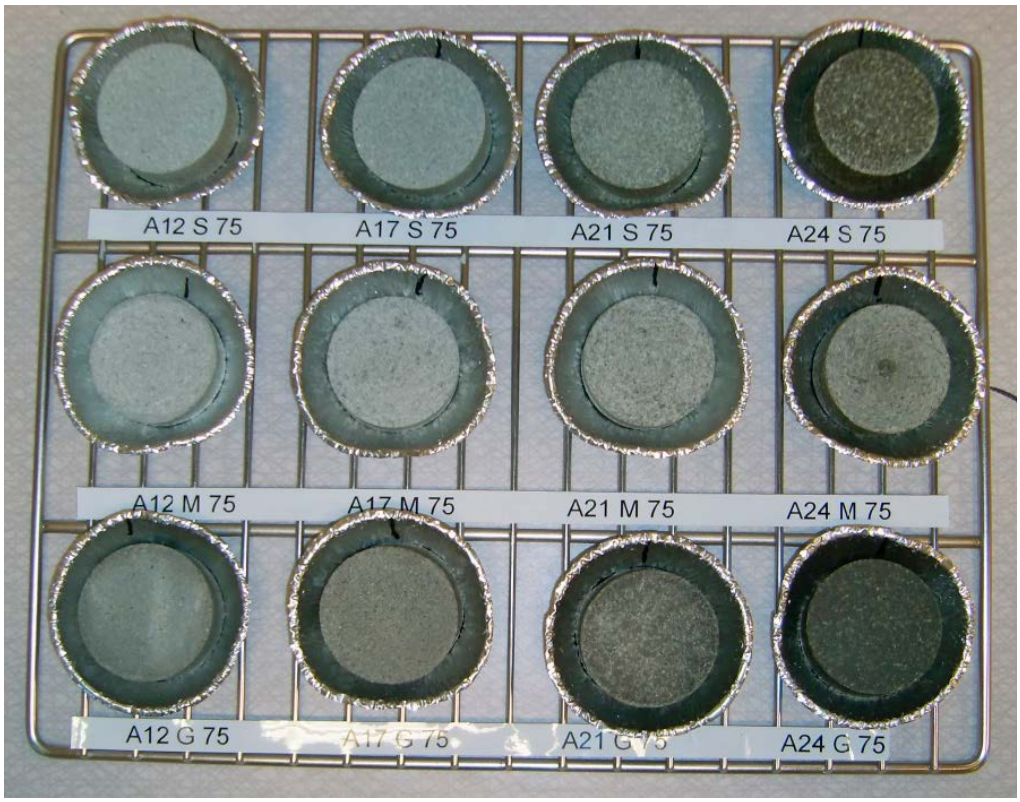

A13-5. *The A specimens before the 75 % Rh test.*

A13-6. *The A specimens after the 75 % Rh test.*

A13-7. *The B specimens before the 75 % Rh test.*

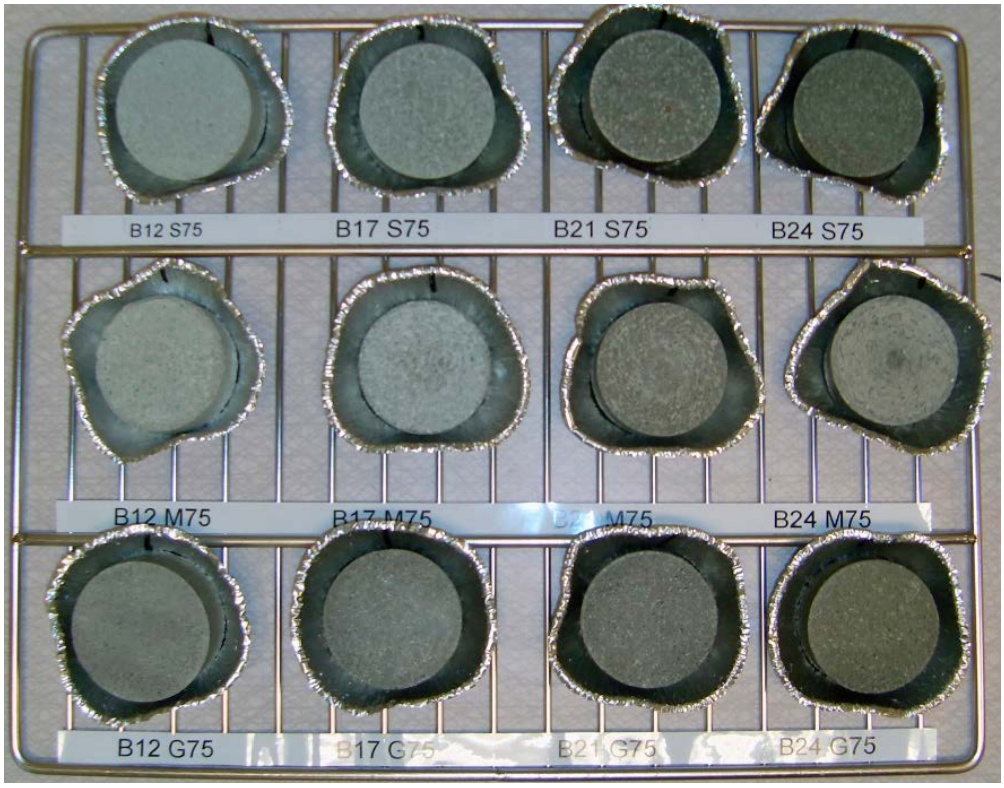

A13-8. *The B specimens after the 75 % Rh test.*

A13-9. *The A specimens before the 95 % Rh test.*

A13-10. *The A specimens after the 95 % Rh test.*

A13-11. *The B specimens before the 95 % Rh test.*

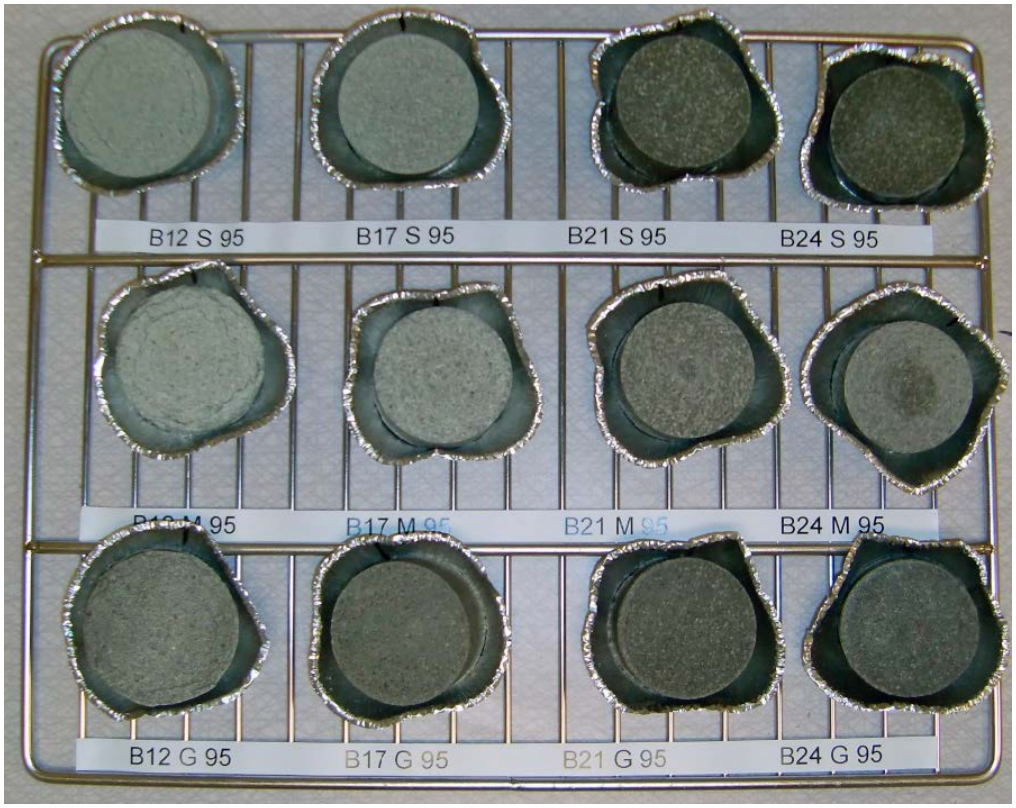

A13-12. *The B specimens after the 95 % Rh test.*

Appendix 14

Table showing all data from the climate tests

		Mass difference			Water ratio determination			Density determination			Volume determination						
Date:	**2014-08-12**	**2014-08-12**	**2014-08-29**	**Time [h]**	**2014-08-29**	**2014-09-01**		**m string**	**0.012**	**g**	**2014-08-12**	**2014-08-12**	**2014-08-29**	**2014-08-29**			
Time:	**08:00**	**08:30**	**15:30**	**415**	**09:30**	**11:00**		**ρ paraffin**	**883.4**	**kg/m³**	**08:30**	**08:30**	**15:30**	**15:30**	**[mm³]**	**[mm³]**	**[%]**
Specimen	**Mass Beaker**	**Mass start**	**Mass end**		**Mass**	**Mass dry**	**W [%]**	**Mass air**	**Mass par**	**ρ [kg/m³]**	**dia [mm]**	**heigth [mm]**	**dia [mm]**	**heigth [mm]**	**Vol start**	**vol end**	**Δvolume**
A12 S 35	0.724	80.332	77.925	−3.02	35.848	33.472	7.26	40.302	21.532	1896.2	49.230	22.850	49.180	22.380	43 495	42 514	−2.3
A17 S 35	0.717	80.192	74.670	−6.95	39.185	36.301	8.10	33.729	18.492	1954.8	49.380	21.390	48.420	20.800	40 964	38 300	−6.5
A21 S 35	0.735	79.875	72.600	−9.19	38.420	35.442	8.58	32.319	18.314	2037.8	49.130	20.710	47.640	19.810	39 261	35 312	−10.1
A24 S 35	0.731	79.680	70.940	−11.07	31.955	29.434	8.78	37.162	21.462	2090.3	48.860	20.690	46.860	19.760	38 793	34 079	−12.2
A12 M 35	0.722	65.430	63.373	−3.18	29.563	27.643	7.13	31.777	16.760	1868.6	48.210	20.020	47.750	19.770	36 545	35 403	−3.1
A17 M 35	0.722	69.766	65.016	−6.88	30.170	28.005	7.94	33.302	18.148	1940.6	47.810	19.970	46.990	19.390	35 851	33 626	−6.2
A21 M 35	0.733	70.396	64.024	−9.15	29.871	27.597	8.46	32.722	18.496	2031.2	47.840	19.240	46.440	18.390	34 584	31 150	−9.9
A24 M 35	0.732	72.362	64.458	−11.03	34.983	32.249	8.67	27.780	16.043	2090.0	48.310	19.100	46.330	18.080	35 010	30 480	−12.9
A12 G 35	0.721	80.826	78.298	−3.16	41.041	38.392	7.03	35.170	18.670	1882.3	49.600	22.200	49.160	21.930	42 895	41 625	−3.0
A17 G 35	0.723	80.490	74.824	−7.10	34.930	32.434	7.87	37.960	21.003	1976.9	49.400	21.030	48.430	20.410	40 307	37 598	−6.7
A21 G 35	0.733	79.910	72.629	−9.20	36.645	33.870	8.37	34.108	19.349	2040.8	49.100	20.640	47.650	19.720	39 081	35 166	−10.0
A24 G 35	0.727	79.491	70.854	−10.97	38.421	35.453	8.55	30.550	17.618	2086.1	48.840	20.610	46.950	19.560	38 612	33 863	−12.3
B12 S 35	0.734	80.551	78.150	−3.01	37.448	34.958	7.28	38.717	21.710	2010.5	49.620	20.800	49.200	20.790	40 222	39 525	−1.7
B17 S 35	0.718	80.203	74.796	−6.80	36.584	33.900	8.09	36.339	20.733	2056.3	49.340	20.250	48.400	19.800	38 718	36 429	−5.9
B21 S 35	0.723	79.960	72.657	−9.22	37.636	34.727	8.55	33.176	19.219	2099.1	48.980	20.180	47.500	19.330	38 023	34 254	−9.9
B24 S 35	0.729	79.546	71.009	−10.83	34.697	31.958	8.77	34.435	19.969	2102.1	48.750	20.460	46.830	19.430	38 190	33 467	−12.4
B12 M 35	0.728	70.800	68.652	−3.07	35.383	33.058	7.19	31.524	17.592	1998.1	48.070	19.630	47.660	19.300	35 625	34 431	−3.4
B17 M 35	0.729	72.259	67.230	−7.74	30.136	27.956	8.01	35.395	20.174	2053.5	47.920	19.350	46.790	18.680	34 898	32 120	−8.0
B21 M 35	0.720	69.038	62.676	−9.31	30.505	28.170	8.51	30.526	17.680	2098.4	47.880	18.310	46.410	17.470	32 968	29 553	−10.4
B24 M 35	0.722	68.682	61.253	−10.93	31.818	29.339	8.66	27.755	16.085	2100.1	46.790	19.050	45.230	18.140	32 756	29 146	−11.0
B12 G 35	0.730	80.899	78.430	−3.08	39.425	36.848	7.13	36.981	20.885	2029.0	49.600	20.550	49.180	20.200	39 707	38 372	−3.4
B17 G 35	0.725	80.455	74.769	−7.13	39.064	36.276	7.84	33.833	19.300	2055.8	49.350	20.300	48.390	19.600	38 829	36 046	−7.2
B21 G 35	0.728	80.085	72.594	−9.44	35.120	32.451	8.41	35.466	20.472	2088.8	49.050	20.240	47.570	19.440	38 245	34 550	−9.7
B24 G 35	0.730	76.159	67.707	−11.21	31.418	28.986	8.61	34.497	20.033	2106.2	48.940	19.810	46.990	18.800	37 265	32 603	−12.5

		Mass difference			Water ratio determination			Density determination			Volume determination						
Date:	**2014-09-01**	**2014-09-01**	**2014-09-15**	**Time [h]**	**2014-09-15**	**2014-09-16**		**m string**	**0,012**	**g**	**2014-09-01**	**2014-09-01**	**2014-09-15**	**2014-09-15**			
Time:	**08:00**	**08:45**	**08:45**	**336**	**11:00**	**11:00**		**ρ paraffin**	**883,4**	**kg/m³**	**08:30**	**08:30**	**15:30**	**15:30**	**[mm³]**	**[mm³]**	**[%]**
Specimen	**Mass Beaker**	**Mass start**	**Mass end**		**Mass**	**Mass dry**	**W [%]**	**Mass air**	**Mass par**	**ρ [kg/m³]**	**dia [mm]**	**heigth [mm]**	**dia [mm]**	**heigth [mm]**	**Vol start**	**vol end**	**Δvolume**
A12 S 75	0.735	80.604	84.005	4.26	49.760	43.361	15.01	30.343	15.445	1798.6	49.47	22.38	50.84	23.71	43 016	48 132	11.9
A17 S 75	0.735	80.059	80.464	0.51	39.109	33.719	16.34	39.123	21.547	1965.8	49.23	21.19	49.36	21.36	40 335	40 873	1.3
A21 S 75	0.736	79.728	79.111	−0.78	37.668	31.970	18.24	39.424	22.446	2050.7	48.95	20.75	48.82	20.52	39 049	38 412	−1.6
A24 S 75	0.733	79.480	77.767	−2.18	39.075	32.945	19.03	36.665	21.293	2106.4	48.69	20.48	48.05	20.27	38 133	36 756	−3.6
A12 M 75	0.737	66.891	69.625	4.13	46.778	40.817	14.87	17.010	8.777	1823.9	47.88	20.42	49.24	21.47	36 767	40 884	11.2
A17 M 75	0.734	71.018	71.347	0.47	34.755	29.999	16.25	34.628	19.057	1963.9	47.71	20.26	47.85	20.21	36 220	36 343	0.3
A21 M 75	0.738	68.096	67.653	−0.66	34.519	29.324	18.17	31.335	17.831	2049.1	47.68	18.52	47.55	18.54	33 068	32 923	−0.4
A24 M 75	0.737	71.184	69.602	−2.25	33.052	27.908	18.93	34.691	20.145	2106.1	47.35	19.24	46.78	19.07	33 879	32 776	−3.3
A12 G 75	0.739	81.015	84.291	4.08	41.167	35.973	14.74	36.622	18.820	1816.7	49.48	22.14	50.77	23.24	42 572	47 048	10.5
A17 G 75	0.734	80.357	80.747	0.49	40.728	35.155	16.19	38.013	21.155	1991.4	49.25	21.03	49.37	21.08	40 063	40 354	0.7
A21 G 75	0.736	80.149	79.438	−0.90	37.467	31.837	18.10	39.905	22.762	2055.8	49.01	20.68	48.80	20.63	39 013	38 586	−1.1
A24 G 75	0.735	79.258	77.672	−2.02	37.109	31.339	18.85	38.577	22.391	2104.8	48.60	20.53	48.09	20.25	38 085	36 781	−3.4
B12 S 75	0.720	80.526	83.897	4.22	39.862	34.754	15.01	41.916	22.522	1908.8	49.49	20.81	50.86	22.02	40 031	44 736	11.8
B17 S 75	0.718	80.094	80.572	0.60	38.159	32.843	16.55	40.370	23.183	2074.4	49.22	20.31	49.32	20.25	38 644	38 687	0.1
B21 S 75	0.722	79.794	79.317	−0.60	37.801	32.007	18.52	39.490	23.029	2118.7	48.79	20.36	48.64	20.21	38 065	37 553	−1.3
B24 S 75	0.723	79.502	77.849	−2.10	36.918	31.120	19.07	38.933	22.714	2119.9	48.61	20.37	48.04	20.03	37 804	36 306	−4.0
B12 M 75	0.720	69.716	72.569	4.14	39.388	34.912	13.09	27.736	15.056	1931.5	47.83	19.36	49.22	20.37	34 785	38 758	11.4
B17 M 75	0.724	73.632	74.022	0.53	35.247	30.386	16.39	36.881	21.118	2066.3	47.70	19.89	47.84	19.68	35 544	35 375	−0.5
B21 M 75	0.724	69.007	68.681	−0.48	33.355	28.273	18.45	33.540	19.568	2119.9	47.74	18.21	47.63	17.97	32 596	32 018	−1.8
B24 M 75	0.722	70.784	69.234	−2.21	33.558	28.310	19.02	33.856	19.745	2118.8	47.51	19.05	46.64	18.81	33 772	32 136	−4.8
B12 G 75	0.720	80.831	84.151	4.14	46.770	40.832	14.80	32.902	17.870	1932.9	49.45	20.36	50.82	21.71	39 102	44 037	12.6
B17 G 75	0.722	80.358	80.761	0.51	38.303	33.014	16.38	40.145	23.049	2073.8	49.21	20.22	49.32	20.25	38 457	38 687	0.6
B21 G 75	0.722	79.962	79.340	−0.78	38.098	32.310	18.32	39.228	22.836	2113.5	48.86	20.24	48.69	20.02	37 950	37 276	−1.8
B24 G 75	0.714	78.737	76.921	−2.33	37.392	31.570	18.87	37.552	21.854	2112.6	48.70	20.32	48.05	19.98	37 850	36 230	−4.3

		Mass difference			Water ratio determination			Density determination			Volume determination						
Date:	**2014-09-16**	**2014-09-16**	**2014-10-02**	**Time [h]**	**2014-10-02**	**2014-10-02**		**m string**	**0,012**	**g**	**2014-09-16**	**2014-09-16**	**2014-10-02**	**2014-10-02**			
Time:	**08:00**	**08:00**	**09:00**	**385**	**11:00**	**11:00**		**ρ paraffin**	**883,4**	**kg/m³**	**08:00**	**08:00**	**15:30**	**15:30**	**[mm³]**	**[mm³]**	**[%]**
Specimen	**Mass Beaker**	**Mass start**	**Mass end**		**Mass**	**Mass dry**	**W [%]**	**Mass air**	**Mass par**	**ρ [kg/m³]**	**dia [mm]**	**heigth [mm]**	**dia [mm]**	**heigth [mm]**	**Vol start**	**vol end**	**Δvolume**
A12 S 95	0.734	80.539	89.932	11.77	57.194	46.619	23.05	12.191	6.040	1749.2	49.44	22.47	53.39	25.99	43 137	58 186	34.9
A17 S 95	0.733	79.996	85.504	6.95	40.631	33.039	23.50	42.333	22.345	1870.5	49.23	21.20	51.71	22.71	40 354	47 693	18.2
A21 S 95	0.737	79.606	82.903	4.18	40.600	32.934	23.81	40.302	22.251	1971.8	48.93	20.68	50.18	21.49	38 886	42 500	9.3
A24 S 95	0.735	79.299	81.434	2.72	40.398	32.590	24.51	39.027	21.951	2018.4	48.55	20.48	49.56	21.07	37 914	40 646	7.2
A12 M 95	0.736	68.230	76.139	11.72	44.601	36.394	23.02	20.593	10.110	1734.4	47.81	21.08	51.93	24.37	37 844	51 616	36.4
A17 M 95	0.735	72.751	77.689	6.86	38.292	31.179	23.36	37.638	19.878	1871.6	47.65	20.44	49.57	21.88	36 450	42 226	15.8
A21 M 95	0.731	68.720	71.654	4.32	35.353	28.723	23.69	34.578	19.070	1969.0	47.74	18.60	49.00	19.47	33 294	36 715	10.3
A24 M 95	0.729	71.940	73.811	2.63	36.563	29.528	24.43	35.394	19.940	2022.6	47.72	19.28	48.43	19.77	34 482	36 419	5.6
A12 G 95	0.734	80.698	90.034	11.68	54.142	44.174	22.95	20.037	9.950	1753.8	49.47	22.03	53.38	25.70	42 344	57 515	35.8
A17 G 95	0.733	80.393	85.772	6.75	42.715	34.815	23.18	40.465	21.120	1847.3	49.23	21.41	51.25	23.00	40 754	47 447	16.4
A21 G 95	0.733	79.808	83.013	4.05	41.325	33.581	23.58	39.577	21.904	1977.7	48.92	20.57	50.20	21.44	38 663	42 435	9.8
A24 G 95	0.732	79.178	81.335	2.75	39.390	31.821	24.35	39.906	22.482	2022.7	48.55	20.53	49.52	21.19	38 006	40 811	7.4
B12 S 95	0.731	80.591	89.706	11.41	59.357	48.448	22.86	23.088	11.678	1786.7	49.46	20.67	53.35	24.45	39 714	54 656	37.6
B17 S 95	0.734	80.067	85.300	6.60	42.205	34.401	23.18	40.945	22.322	1941.7	49.16	20.24	51.03	21.78	38 417	44 545	16.0
B21 S 95	0.734	79.623	82.873	4.12	40.008	32.481	23.71	40.859	23.069	2028.4	48.71	20.02	50.00	21.00	37 307	41 233	10.5
B24 S 95	0.733	79.313	80.981	2.12	38.751	31.441	23.80	40.216	22.856	2045.9	48.52	20.33	49.24	20.85	37 590	39 704	5.6
B12 M 95	0.732	71.210	79.278	11.45	43.606	35.654	22.77	21.359	10.850	1794.5	47.91	19.39	51.74	22.75	34 956	47 833	36.8
B17 M 95	0.735	71.074	75.731	6.62	35.946	29.303	23.25	37.801	20.557	1935.9	47.70	18.96	49.51	20.51	33 882	39 486	16.5
B21 M 95	0.733	72.100	75.010	4.08	37.434	30.359	23.88	35.734	20.132	2022.6	47.62	19.01	48.90	19.79	33 857	37 167	9.8
B24 M 95	0.734	69.639	71.463	2.65	34.796	28.074	24.59	34.881	19.741	2034.6	47.09	18.82	48.22	19.35	32 777	35 337	7.8
B12 G 95	0.729	80.677	89.783	11.39	66.539	54.356	22.72	11.435	5.790	1787.7	49.46	20.54	53.20	24.20	39 464	53 793	36.3
B17 G 95	0.729	80.324	85.484	6.48	42.567	34.707	23.13	40.509	22.075	1940.7	49.18	20.18	51.08	21.85	38 334	44 776	16.8
B21 G 95	0.729	79.735	82.810	3.89	40.378	32.777	23.72	40.384	22.746	2022.1	48.83	20.12	50.03	21.21	37 678	41 696	10.7
B24 G 95	0.727	79.383	81.250	2.37	40.071	32.356	24.39	39.185	22.143	2030.6	48.62	20.41	49.46	21.08	37 893	40 501	6.9

Arkitektkopia AB, Bromma, 2016

SKB is tasked with managing Swedish nuclear and radioactive waste in a safe way.

skb.se